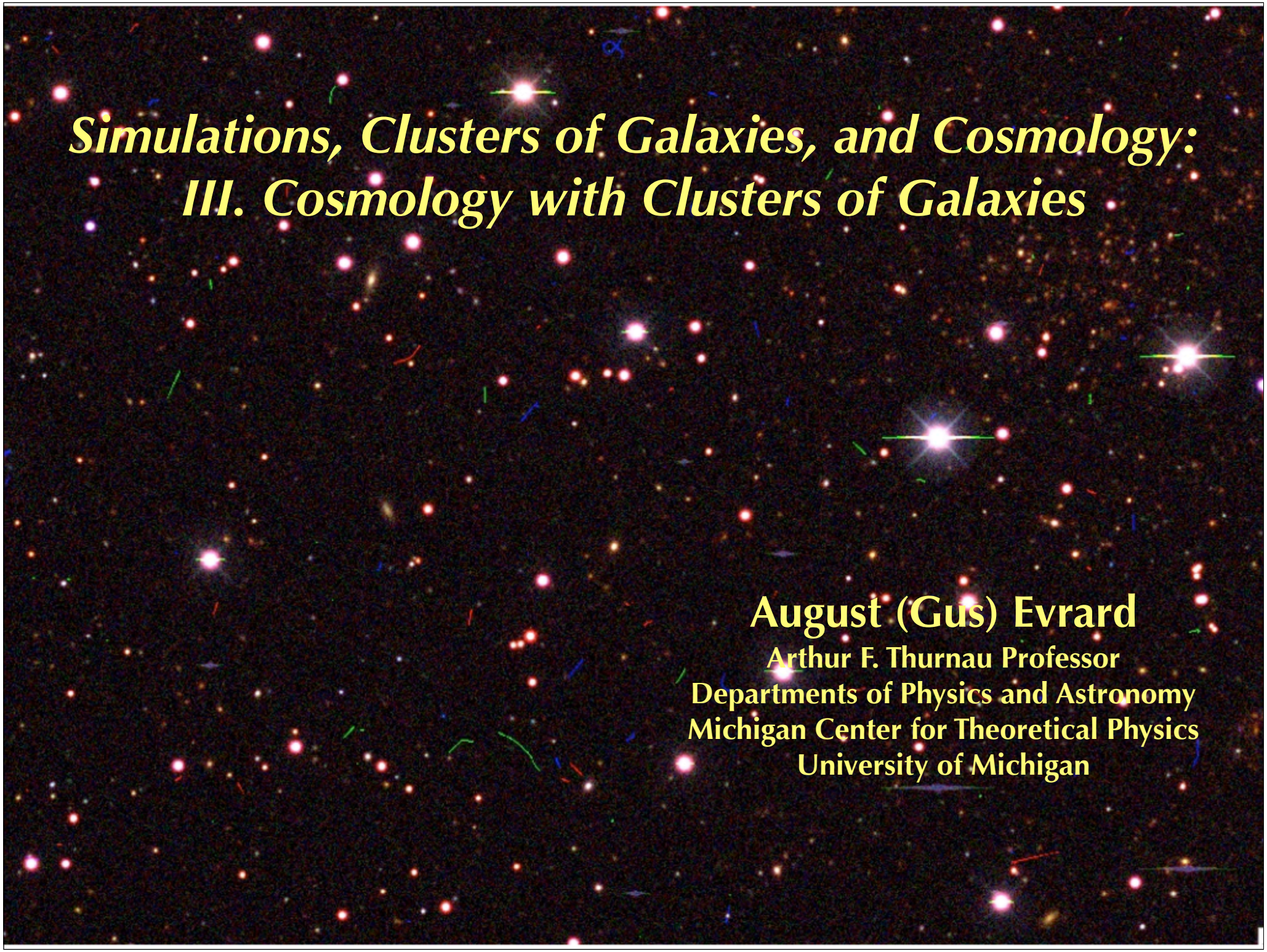

Simulations, Clusters of Galaxies, and Cosmology: III. Cosmology with Clusters of Galaxies

August (Gus) Evrard
Arthur F. Thurnau Professor
Departments of Physics and Astronomy
Michigan Center for Theoretical Physics
University of Michigan

the lexicon

*** Halo :**

a self-bound, quasi-equilibrium structure comprised of multiple, interacting fluids (dark matter, multi-phase baryons, and radiation) formed via gravitational collapse within a cosmic web of random noise.

*** Cluster :**

a redshift-space projection of a massive halo, *and its line-of-sight neighbors*, with the resultant system containing multiple, bright galaxies and other visible components (multi-phase baryons, non-thermal matter, etc.).

massive halo phenomenology: observable signal likelihoods

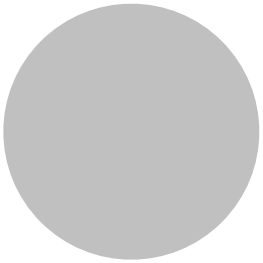

halo of
mass M
redshift z

=>

optical/lensing **sub-mm** **X-ray**

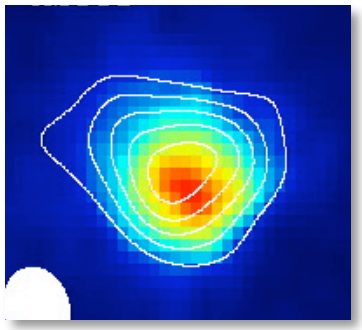

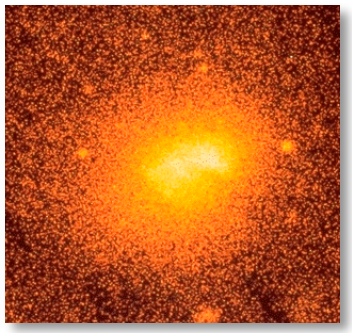

"Astrophysics 101"

1. Dimensional analysis => mean relations are power-laws

2. Central Limit Theorem => deviations are log-normal

X-ray scaling behavior of nearby clusters

Pratt et al (2009)

REXCESS sample analysis

- 31 nearby (z<0.2) X-ray selected clusters (from ROSAT REFLEX survey)
- selected to be approx. volume-limited sample
- all re-observed with XMM-Newton satellite moderate exposures

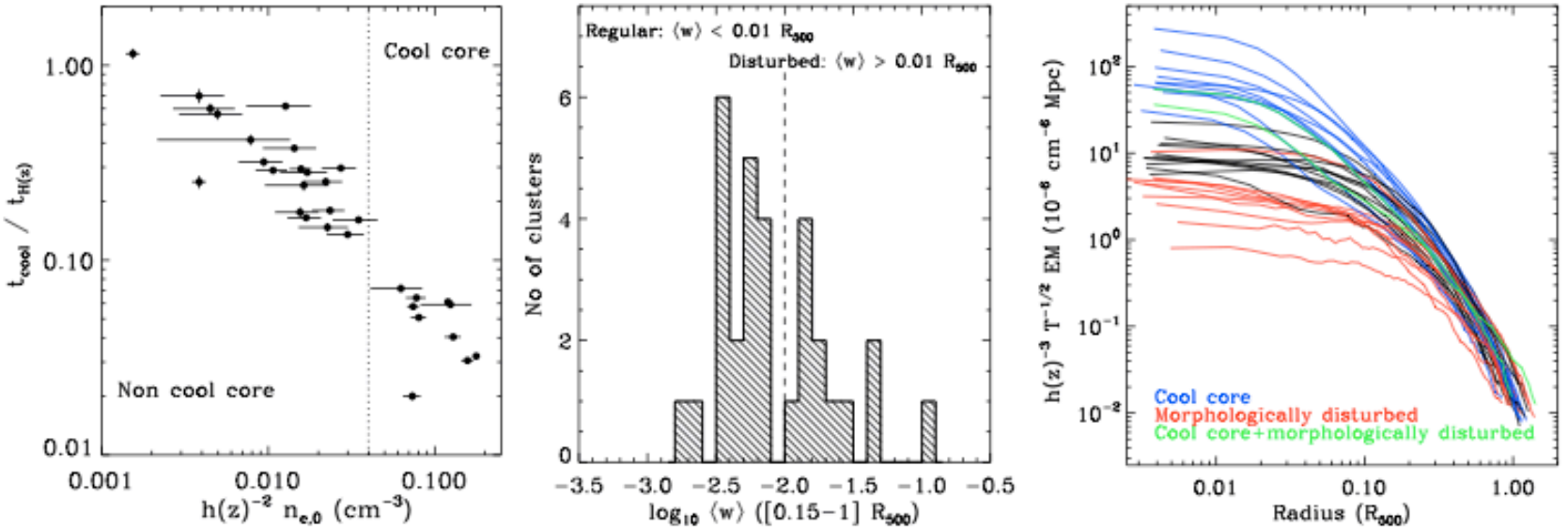

Fig. 1. Definition of cluster subsamples. *Left*: central cooling time vs. central gas density, $n_{e,0}$. The dotted line delineates the threshold we use to define cool core systems: $h(z)^{-2}n_{e,0} > 4 \times 10^{-2}$ cm^{-3}, $t_{cool} < 10^{9}$ years. *Centre*: histogram of centre shift parameter $\langle w \rangle$, evaluated in the [0.15–1] R_{500} aperture. Clusters with $\langle w \rangle > 0.01\,R_{500}$ are classified as morphologically disturbed. *Right*: emission measure profiles of the REXCESS sample, scaled according to the standard dependence on temperature and expected evolution with redshift. Systems classified as cool core and as morphologically disturbed are indicated (see Sect. 2.3).

X-ray scalings are consistent with PL + ~log-normal scatter

REXCESS sample analysis
– luminosity-temperature scaling using full L_X

Pratt et al (2009)

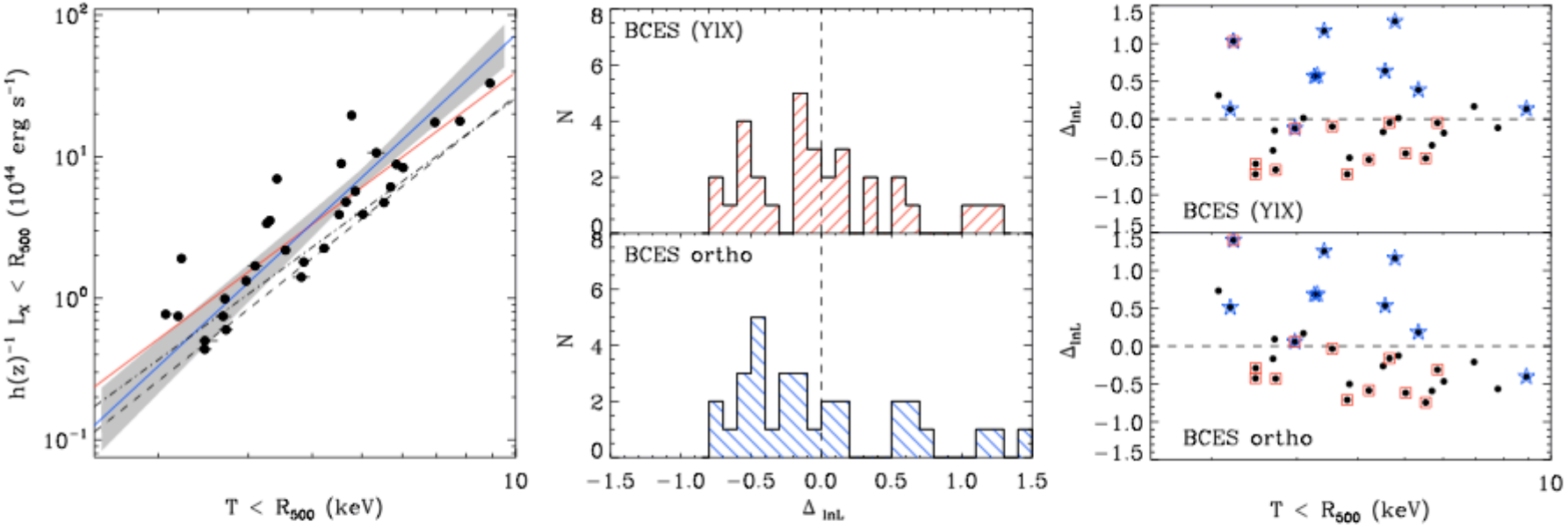

Fig. 2. *Left*: L_1–T_1 relation for the REXCESS sample (quantities derived from all emission interior to R_{500}). The error bars are smaller than the points in many cases. The best fitting power law relation derived from the BCES (Y|X) (red line) and BCES orthogonal (blue line) are overplotted; the shaded region corresponds to the 1σ uncertainty on the latter. The dashed and dot-dashed lines are the relations of Arnaud & Evrard (1999) and Markevitch (1998), respectively. *Centre*: histogram of the log space residuals from the best fitting *L*–*T* relation, derived from each fitting method as indicated. *Right*: Log space residuals for both fitting methods as indicated. Cooling core clusters (blue stars) and morphologically disturbed clusters (red squares) occupy two distinct regions in the plot in both cases.

X-ray scalings: core emission makes dominant contribution to scatter

REXCESS sample analysis

Pratt et al (2009)

– luminosity-temperature scaling using *core-excised* L_X

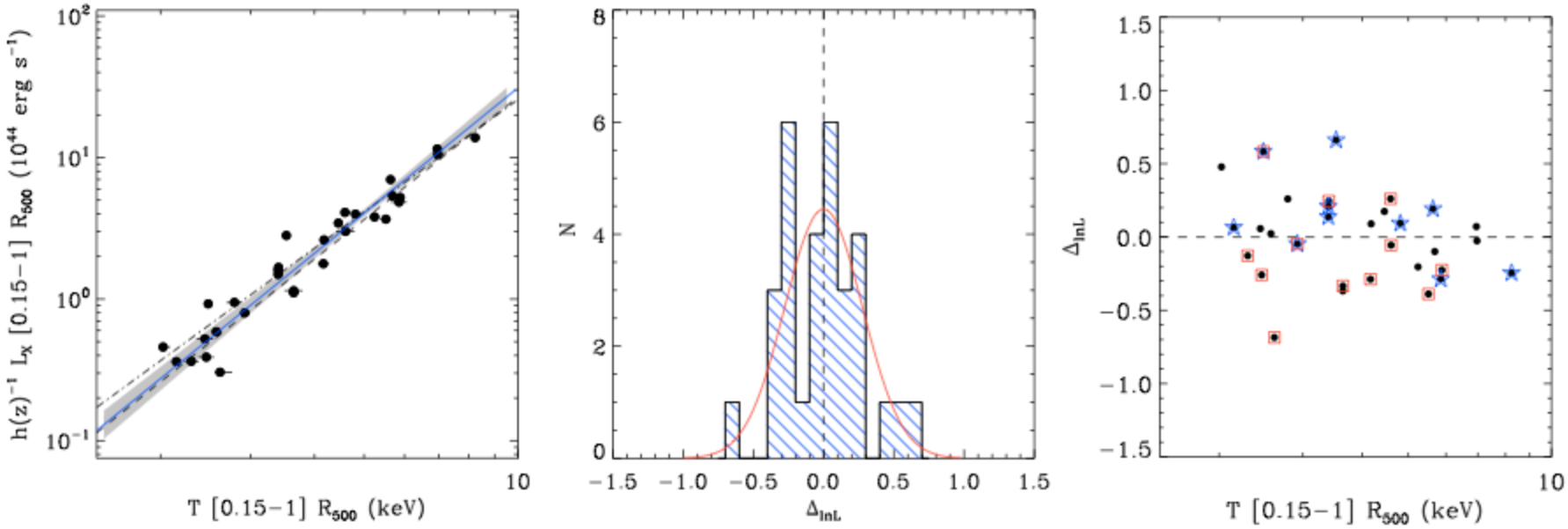

Fig. 3. *Left*: L_2–T_2 relation for the REXCESS sample (quantities derived from emission in the 0.15 R_{500} < R < R_{500} aperture). The best fitting power law relation derived from the BCES orthogonal fitting method is overplotted as a solid line (the BCES (Y|X) results are very similar); the shaded region corresponds to the 1σ uncertainty on the fit. The dashed and dot-dashed lines are the relations of Arnaud & Evrard (1999) and Markevitch (1998), respectively. *Centre*: histogram of the log space residuals from the best fitting L–T relation, derived from the BCES orthogonal fit method. The solid curve is a Gaussian with $\sigma_{\ln L}$ = 0.28, corresponding to the scatter about the best fitting relation. *Right:* Log space residuals. Cooling core clusters (blue stars) and morphologically disturbed clusters (red squares) are less obviously segregated once the central region is excised.

X-ray scalings: minimal scatter between Lx and Yx outside core

REXCESS sample analysis
– core-excised luminosity-Y_X scaling
($Y_X = M_{gas} T_X$ = ICM thermal energy)

Pratt et al (2009)

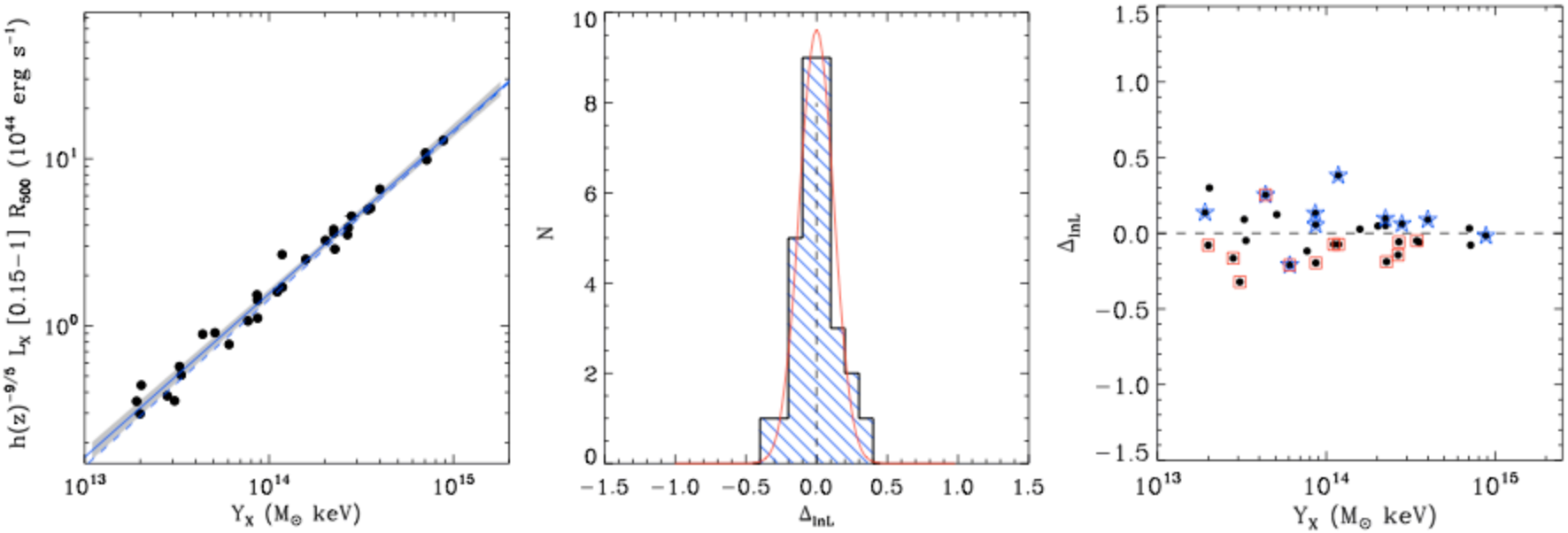

Fig. 5. *Left*: L_2–Y_X relation for the REXCESS sample, with luminosity derived from emission in the $0.15\,R_{500} < R < R_{500}$ aperture. The best fitting power law relation derived from the BCES orthogonal fitting method, which takes into account errors in both coordinates and intrinsic scatter in the data, is overplotted as a solid line (the BCES (Y|X) results are very similar); the shaded region corresponds to the 1σ uncertainty on the fit. The dashed line is the fit derived by Maughan (2007) from observations of 115 galaxy clusters in the *Chandra* archive. The agreement is again excellent. *Centre*: histogram of the log space residuals about the best fitting orthogonal BCES relation. The solid curve is a Gaussian with $\sigma_{\ln L} = 0.16$, corresponding to the scatter about the relation. *Right*: Log space residuals of the different subsets. Blue stars: cooling core clusters, red squares: morphologically disturbed systems.

X-ray scalings: gas mass fraction runs with halo mass

REXCESS sample analysis

– note: total masses estimated from prior M-T scaling

Pratt et al (2009)

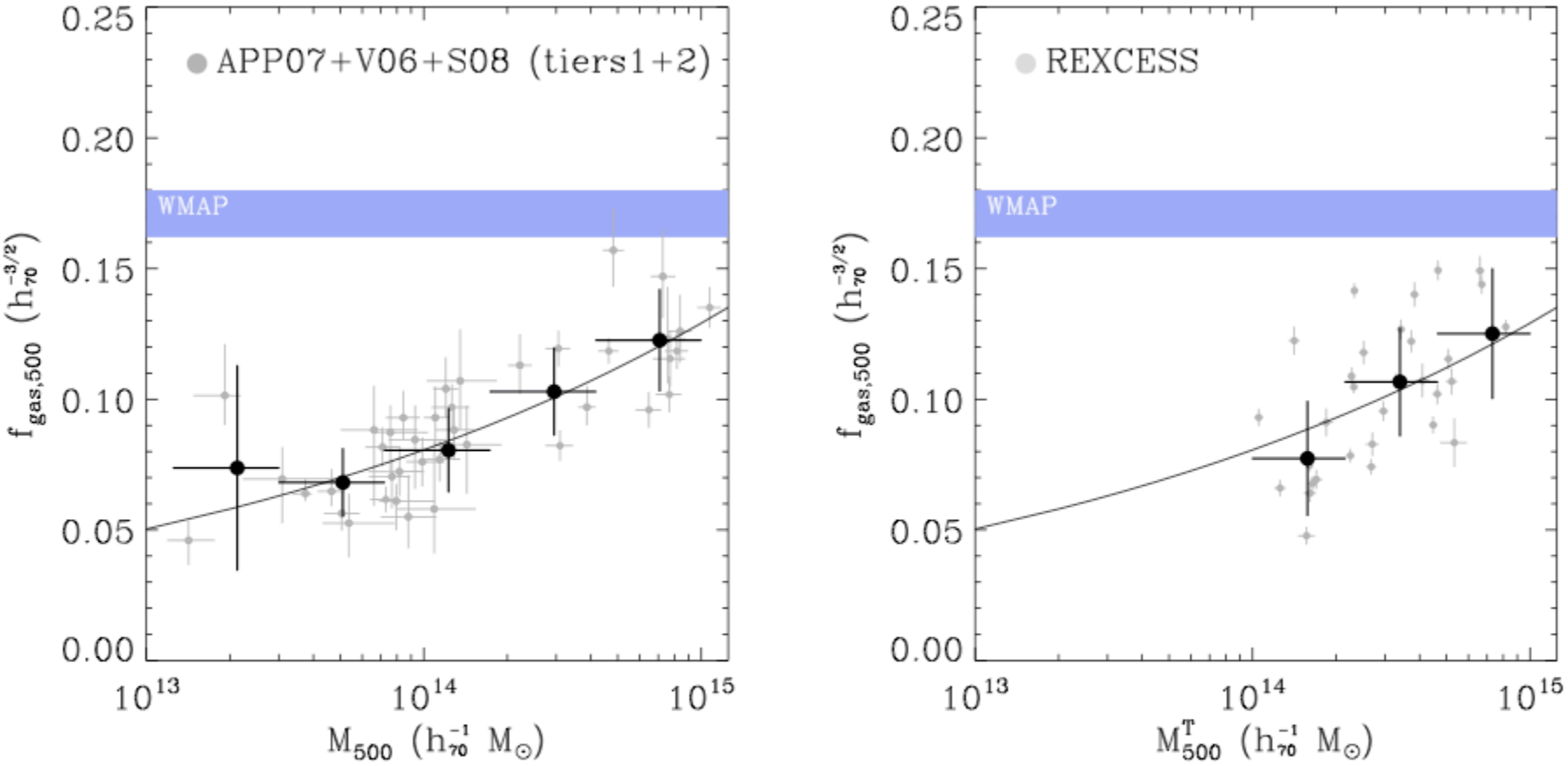

Fig. 8. Gas mass fraction vs mass. *Left panel*: trend of gas mass fraction versus mass derived from X-ray measurements of 41 groups and clusters with high quality hydrostatic mass estimates (Arnaud et al. 2007; Vikhlinin et al. 2006; Sun et al. 2008). Grey points are actual measurements; black points are mean values in logarithmic mass bins. The solid line is the orthogonal BCES fit to the unbinned data, $f_{gas,500} \propto M^{0.2}$. *Right panel*: approximate gas mass fraction versus mass measurements for the REXCESS sample, where the masses have been estimated from the $M_{500} - T$ relation of Arnaud et al. (2005). Black points again show the mean trend for three logarithmic mass bins. The solid line is the same as in the left panel. The band illustrates the WMAP 5-Year baryon fraction constraints (Dunkley et al. 2009).

optical scaling using stacking of similar-richness clusters

maxBCG sample analysis

Johnston et al (2007)
Sheldon et al (2007)

~13000 nearby (0.1<z<0.3) optically selected clusters from Sloan Digital Sky Survey (SDSS)

– richness N_{200} is number of bright, red galaxies within r_{200}

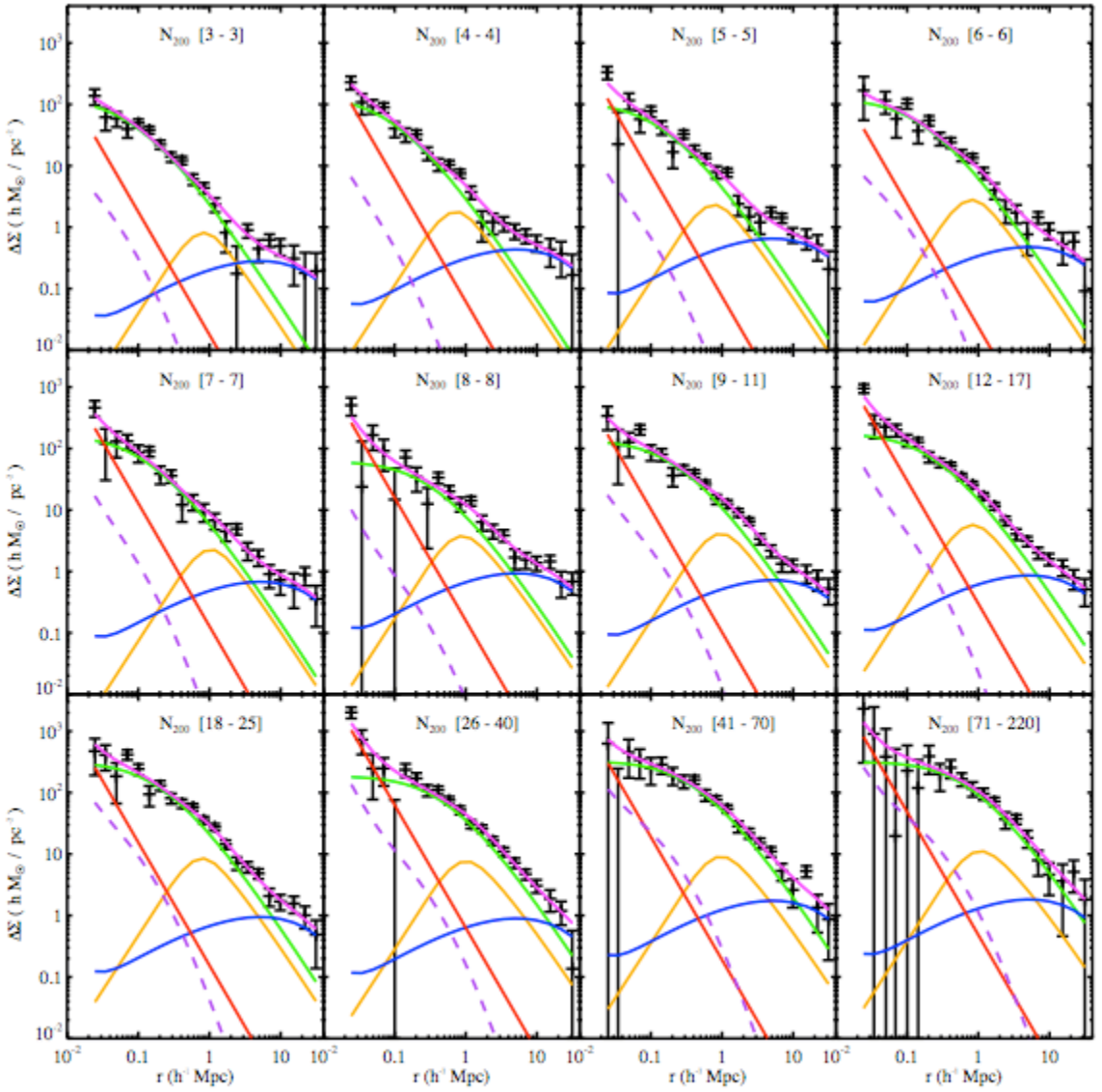

FIG. 8.— Model fits to $\Delta\Sigma(R)$ for the 12 N_{200} richness bins The model components are the NFW halo profile (green), miscentered halo component (orange), the central BCG (red), neighboring halos (blue); the non-linear contribution (purple dashed). The magenta curves

optical scaling using stacking of similar-richness clusters

maxBCG sample analysis

Johnston et al (2007)
Sheldon et al (2007)

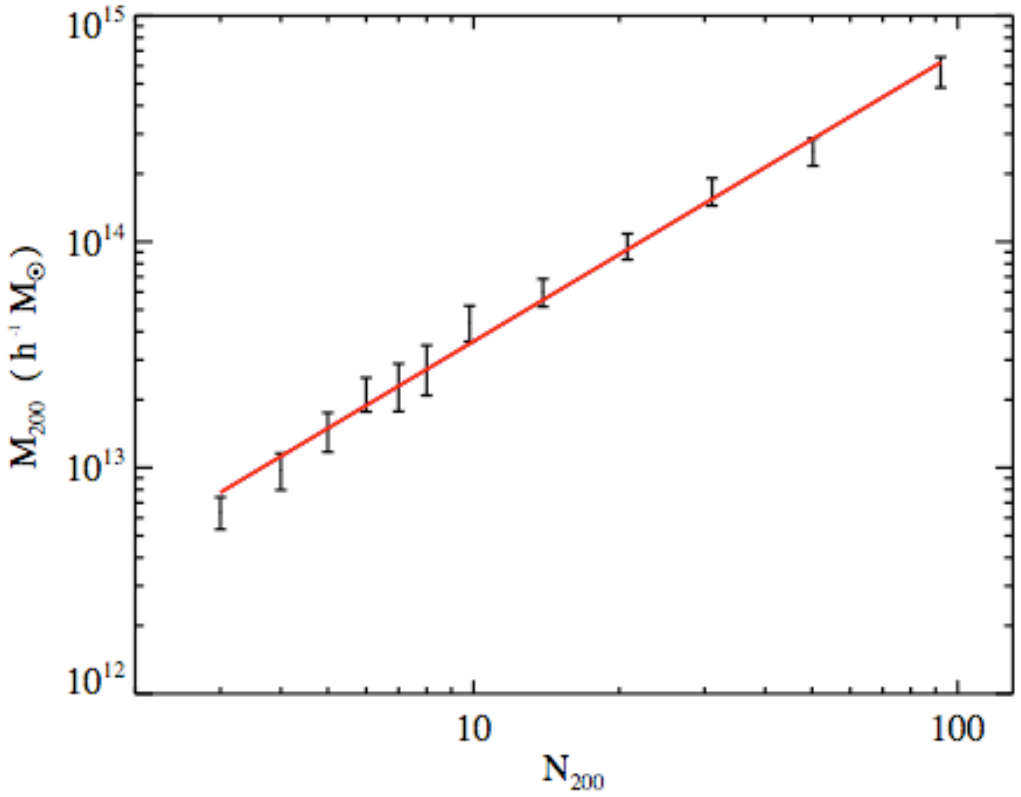

Lx-Mass scaling relation from SDSS maxBCG lensing + RASS

17000 clusters, $N_{gal} \geq 9$

M_{200} from weak lensing, L_X from RASS (stacked N_{gal} bins)

Johston et al 2007
Rykoff et al 2008

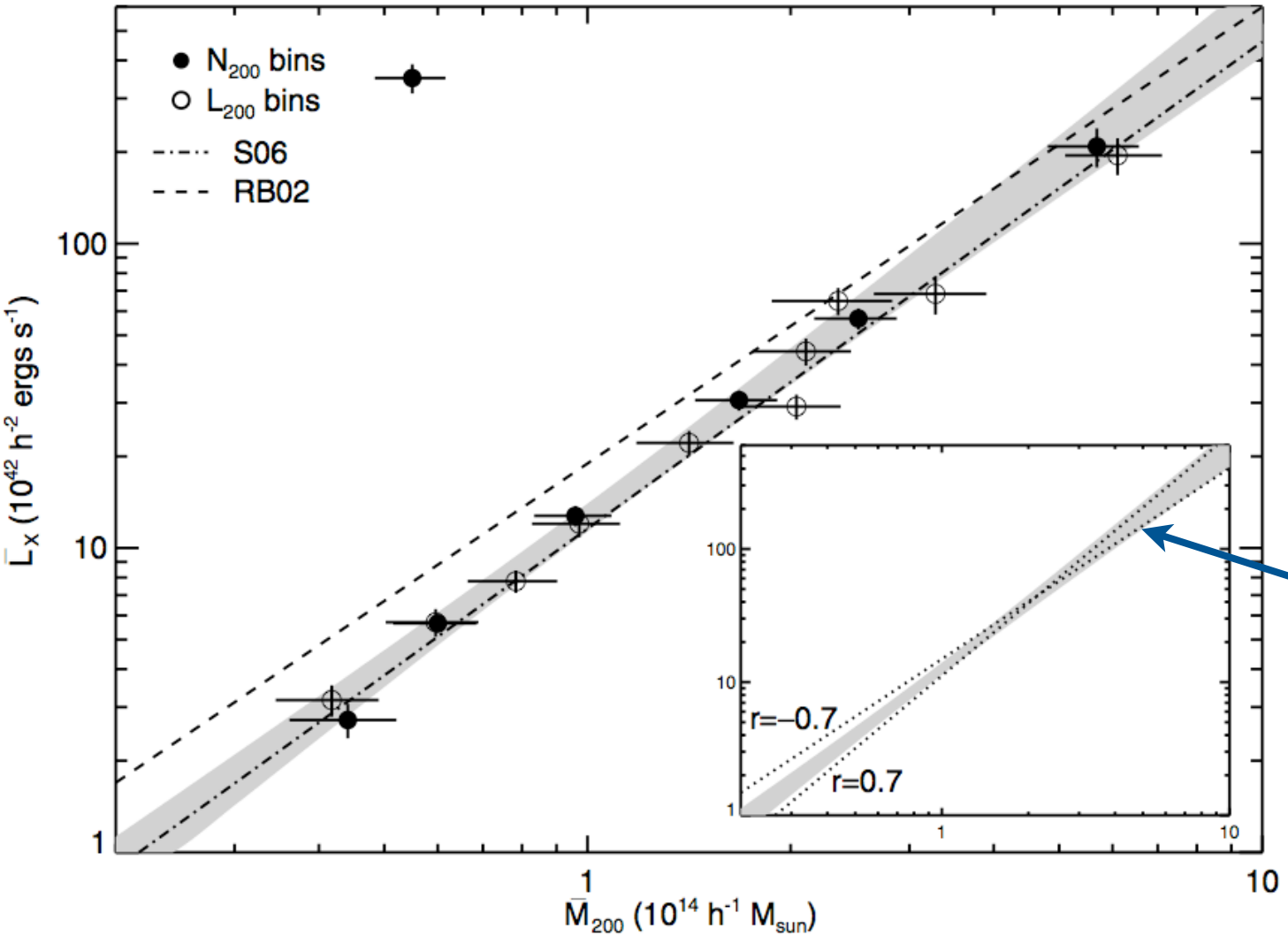

Good agreement between X-ray and optically selected samples
slope = 1.6 ± 0.1

potential ***tilt*** due to intrinsic optical–X-ray correlation

cosmology from counts and clustering of massive halos

brief history of cluster cosmology

* 1933, 36: Zwicky infers the existence of dark matter in the Coma cluster using the virial theorem and ~dozen galaxy velocities

* 1993: the baryon fraction in clusters, coupled with nucleosynthesis limits on the global baryon density, implies a low-density matter parameter, $\Omega_m \approx 0.3$

* 1998: the existence of hot clusters at high redshift (z~0.8) further supports an $\Omega_m \approx 0.3$ model

basic ingredients for cosmology from cluster counts and clustering

1. halo space density (aka, *mass function*), $dn(>M, z)/dV$
   – well calibrated (~5% in dn) by (dark matter only) simulations

2. two-point spatial clustering of halos (aka, *bias function*), $b(M, z)$
   – similarly well calibrated

3. population model for signal, S, used to identify clusters, $p(S \mid M, z)$
   – power-law with log-normal deviations (typically self-calibrated)
   – projection effects (signal-dependent) $S_{observed} \neq S_{intrinsic}$

4. selection model for signal, S
   – completeness (missed clusters)
   – purity (false positives)

expected halo counts above fixed mass of 2e14 Msun/h

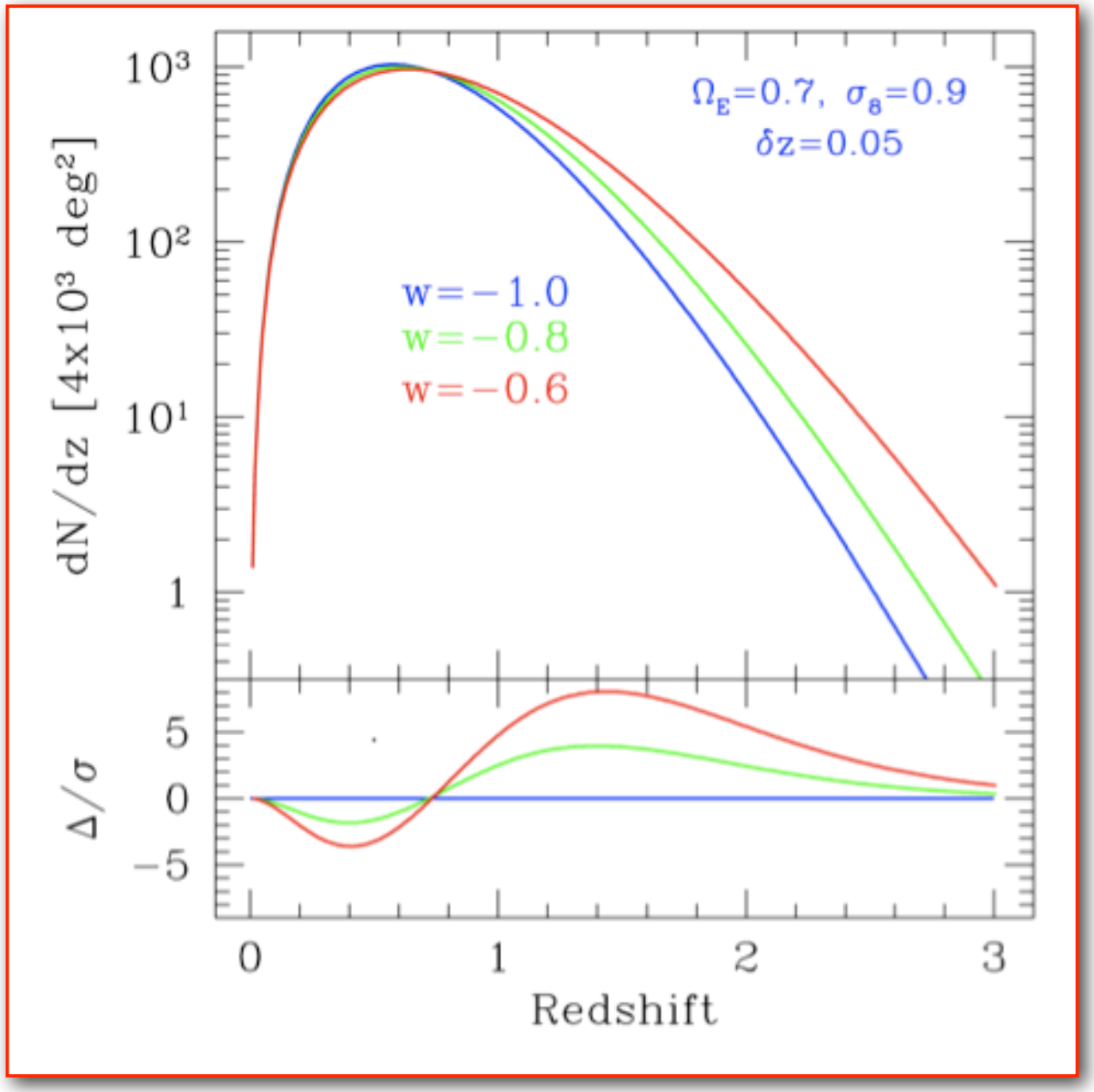

Ruhl et al (2004)

mass-limited sample (formally unobservable)

observable signal choices for surveys: pros and cons

Signal	Pros	Cons
X-ray	• spatially compact signal (relative to other methods) • hot thermal ICM is unique to clusters • 40+ year science history	• expensive (space-based) • flux confusion from AGN • surface brightness dimming • most sources will have moderate S/N
Optical	• inexpensive (*free* with any galaxy survey!) • old, `red sequence' galaxies reside in massive halos • 80+ year science history	• confusion from line-of-sight projection • moderate S/N (Poisson statistics for $N \geq 10$) • galaxy formation!
Sunyaev-Zel'dovich	• inexpensive (*free* with any CMB survey) • nearly redshift-independent signal	• point source confusion • l-o-s projected confusion with low angular resolution • moderate S/N for most

cluster samples today are sparse relative to massive halos on the sky

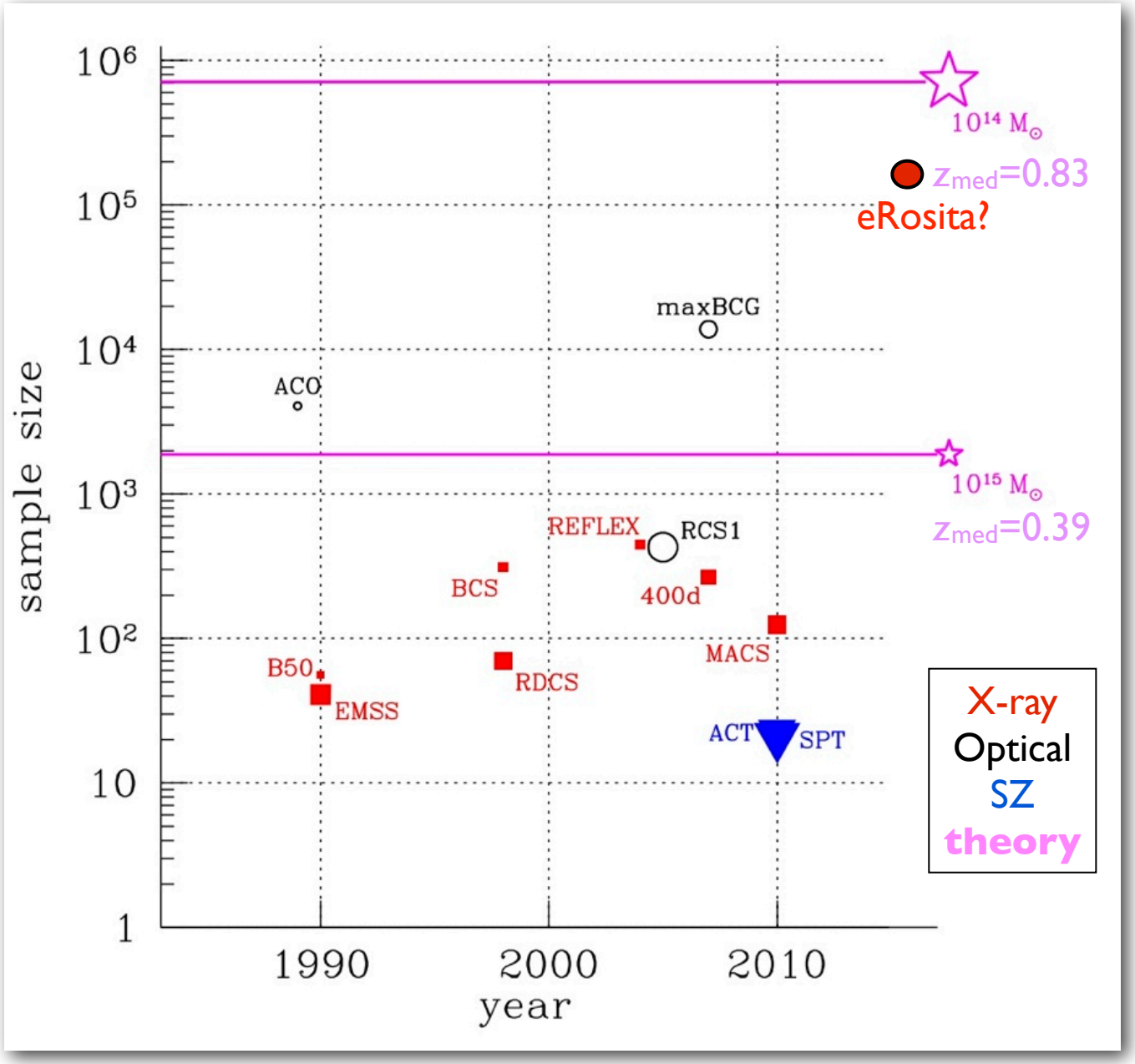

Allen, Evrard & Mantz 2011

symbol size scales with median redshift

Halo mass scale is M_{200m} (h = 0.7)

South Pole Telescope is now operating

SPT is finding distant, massive clusters

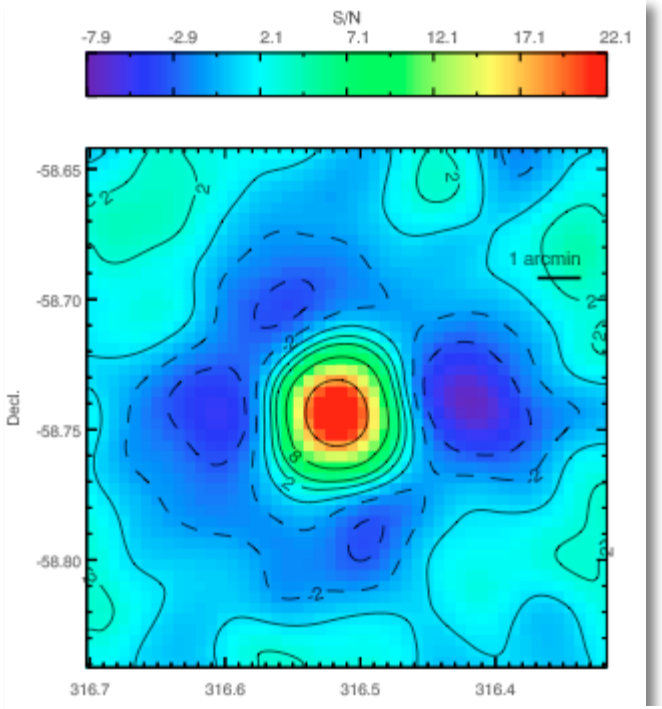

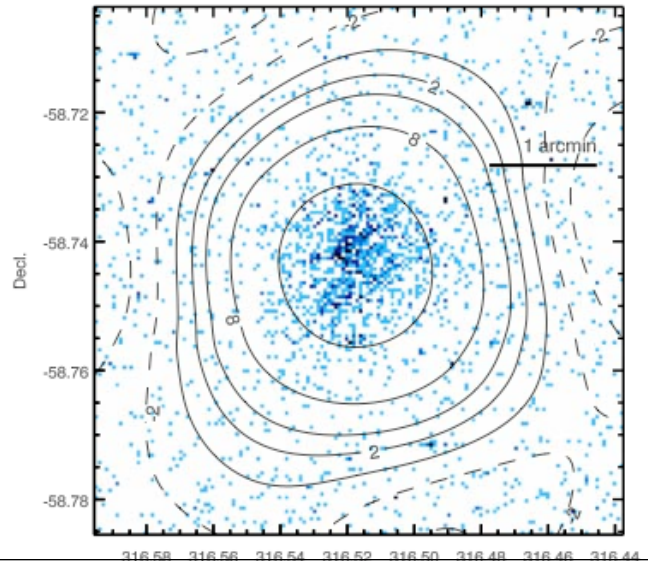

Foley et al, arXiv:1101.1286

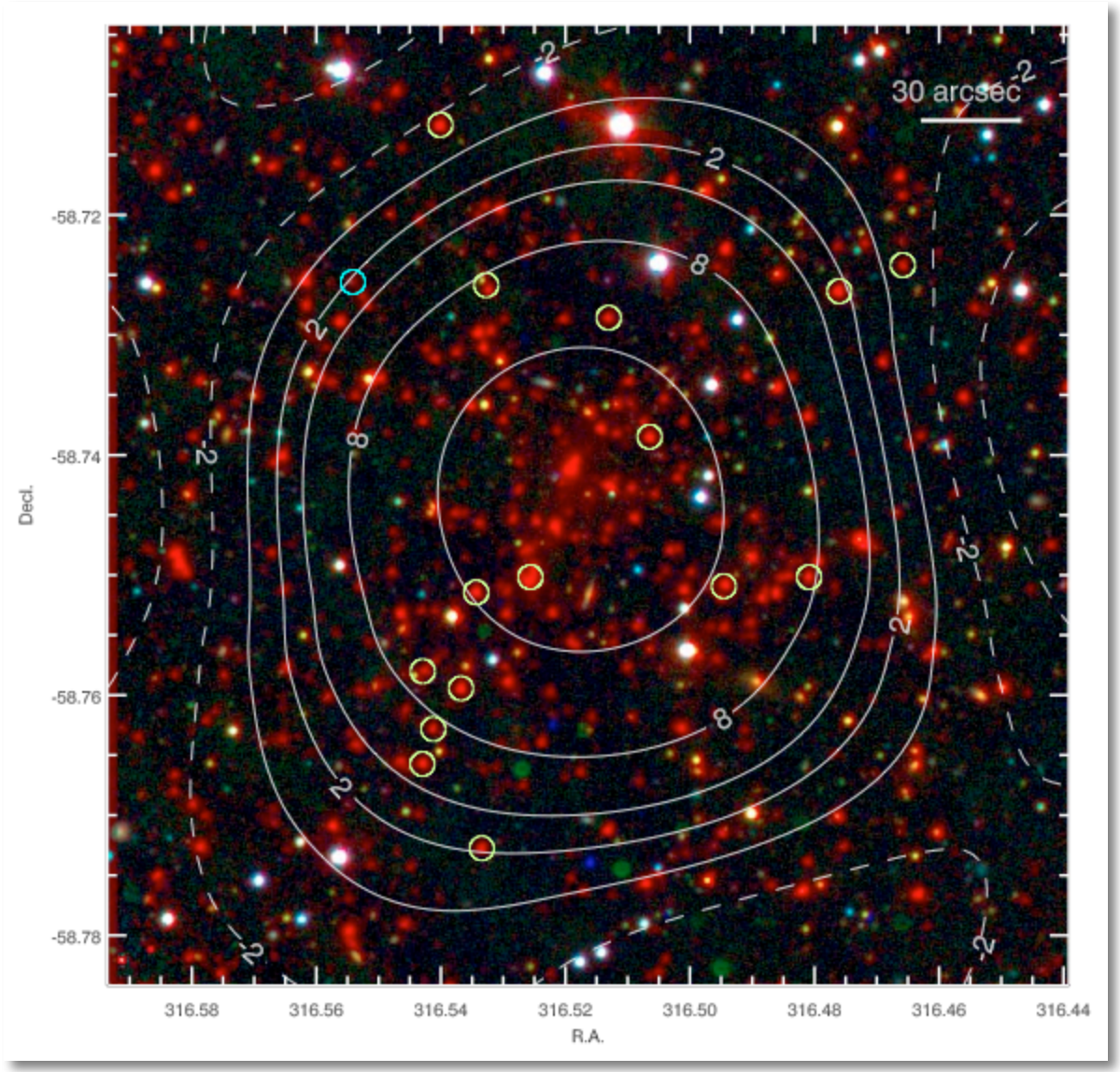

surprise from Planck measurement of maxBCG SZ signal

Planck Collaboration arXiv:1101.2027

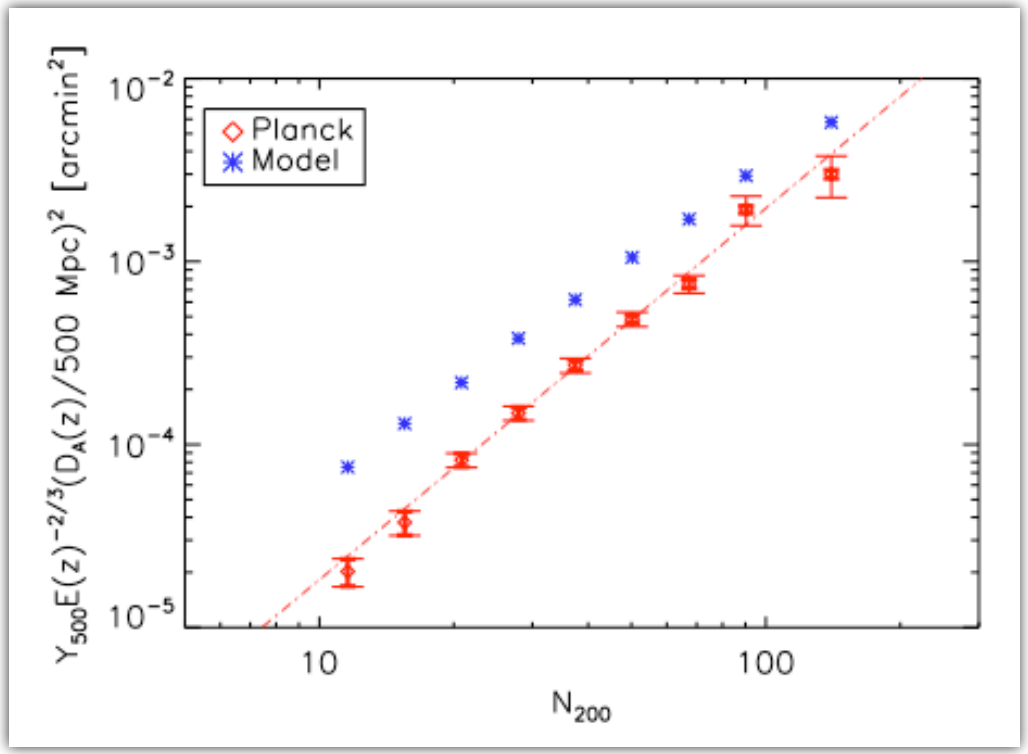

SZ decrement in optically selected clusters smaller than model prediction

Rykoff et al. arXiv:1104.2089

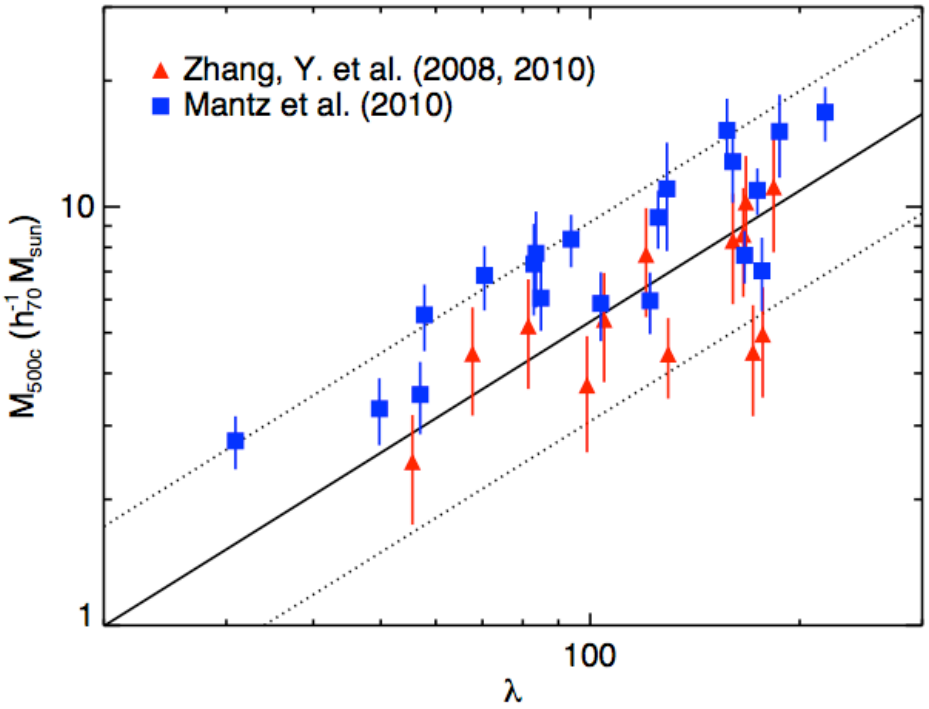

X-ray masses at fixed optical richness differ by ~40% for Chandra vs. XMM analyses

consistent cosmology from existing optical and X-ray samples

Rozo et al 2010

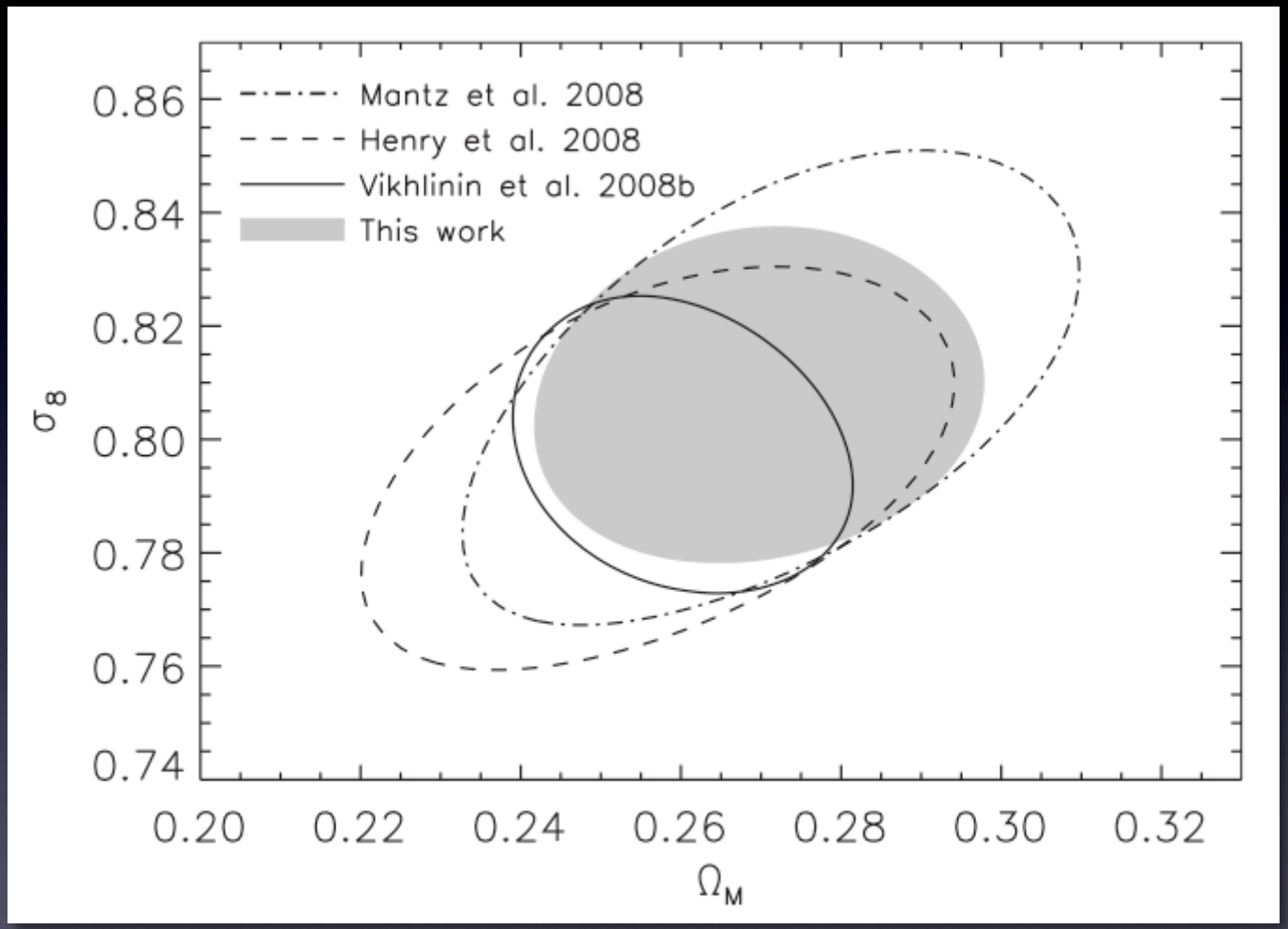

optical: maxBCG
(shaded)
~14,000 clusters

X-ray: 400d, BCS
(lines)
~100 clusters

systematics limited !

how hard is counting? Major systematic error sources for cluster cosmology

1. 3D halo mass is not directly observable
   – what is the form of intrinsic signal likelihood, $p(\boldsymbol{S}_{\rm int} \mid M, z)$?

2. The universe is a big place
   – how does projection along Gpc sight-line chance the observed signal, $\boldsymbol{S}_{\rm obs}$?

$$\boldsymbol{S}_{\rm obs} = \boldsymbol{S}_{\rm int} + \boldsymbol{S}_{\rm proj}$$

3. Baryons (17% of matter) are dynamically complex on Mpc scales
   – how significant are the decaying modes excited by baryon hydrodynamics in LSS formation?

cosmological complementarity from cluster counts + clustering

Cunha, Huterer Frieman, 0904.1589

$$\bar{n}_\alpha(z) \equiv \int_{M_\alpha^{\rm obs}}^{M_{\alpha+1}^{\rm obs}} \frac{dM^{\rm obs}}{M^{\rm obs}} \int \frac{dM}{M} \frac{d\bar{n}}{d\ln M} p(M^{\rm obs}|M)$$

$$p(M^{\rm obs}|M) = \frac{1}{\sqrt{2\pi\sigma^2_{\ln M}}} \exp[-x^2(M^{\rm obs})], \qquad x(M^{\rm obs}) \equiv \frac{\ln M^{\rm obs} - \ln M - \ln M^{\rm bias}(M,z)}{\sqrt{2\sigma_{\ln M}(M,z)^2}}.$$

$$\ln M^{\rm bias}(M_{\rm obs},z) = \ln M_0^{\rm bias} + a_1 \ln(1+z) + a_2(\ln M_{\rm obs} - \ln M_{\rm pivot}) \quad (3)$$

$$\sigma^2_{\ln M}(M_{\rm obs},z) = \sigma_0^2 + \sum_{i=1}^{3} b_i z^i + \sum_{i=1}^{3} c_i (\ln M_{\rm obs} - \ln M_{\rm pivot})^i \quad (4)$$

← *nuisance*:
4 mass bias params
7 mass variance params

PCA analysis of DE figure of merit

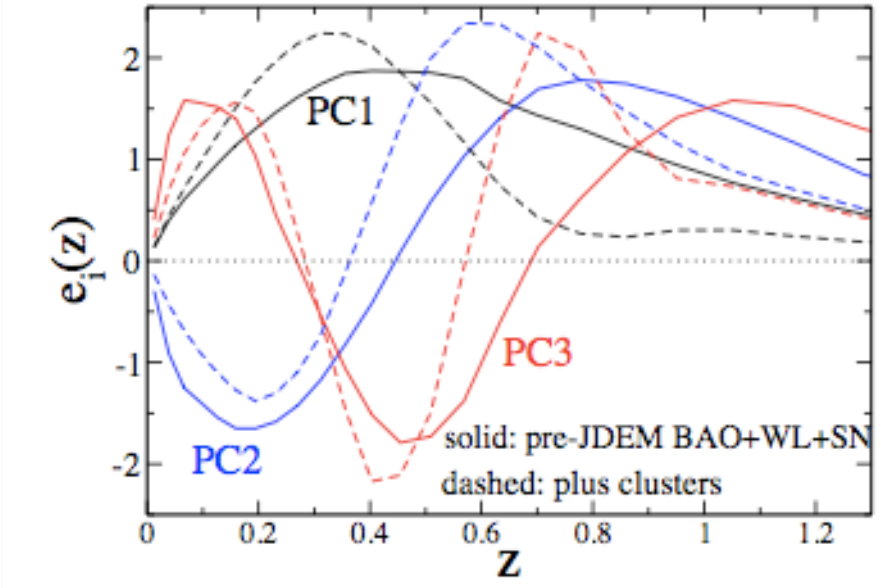

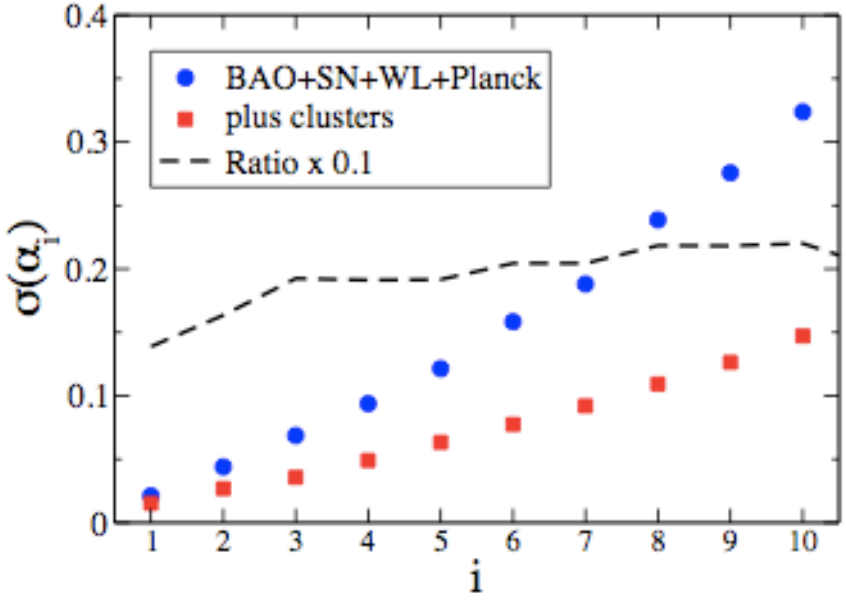

PL+LN covariance model for halo signals

1 A Local Model for Multivariate Counts

Consider a mass function described locally as a power-law in mass with slope $-\alpha$. Specifically, using $\mu \equiv \ln M$, define the mass function, $n(\mu, z)$, as the likelihood of finding a halo at redshift z in the mass range μ to $\mu + d\mu$ within a small comoving volume dV,

$$dp \;\equiv\; n(M,z)\, d\ln M\, dV \;=\; AM^{-\alpha} d\ln M\, dV \;=\; A\, e^{-\alpha\mu}\, d\mu\, dV. \qquad (1)$$

piecewise power-law mass function

The local slope, α, and amplitude, A, implicitly depend on mass and redshift in a manner dependent on cosmology (*e.g.*, Tinker et al. 2008).

Consider a set of N halo properties, $S_i \in \{N_{\rm gal}, L_{\rm X}, T_{\rm X}, M_{\rm gas}, Y_{\rm X}, Y_{\rm SZ}, \cdots\}$, let $\mathbf{s}$ be a vector containing their logarithms,

$$s_i \;=\; \ln(S_i) \qquad (2)$$

Assume that the mass scaling behavior of these properties are power-laws, so that the mean ln(signal) for a mass–complete sample scales as

$$\bar{\mathbf{s}}(\mu, z) \;=\; \mathbf{m}\mu + \mathbf{b}(z). \qquad (3)$$

assumed form of signal-mass relation

The elements of vector $\mathbf{m}$ are the slopes of the individual mass-observable relations. (Note that, at some fixed epoch, we can always choose units such that the intercepts $b_i(z) = 0$.)

Assume that ln(signal) deviations about the mean are Gaussian, described by a likelihood

$$p(\mathbf{s}|\mu) \;=\; \frac{1}{(2\pi)^{N/2}|\Psi|^{1/2}} \exp\left[-\frac{1}{2}(\mathbf{s}-\bar{\mathbf{s}})^{\dagger}\Psi^{-1}(\mathbf{s}-\bar{\mathbf{s}})\right], \qquad (4)$$

where the covariance matrix has elements

$$\Psi_{ij} \equiv \langle (s_i - \bar{s}_i)(s_j - \bar{s}_j)\rangle, \qquad (5)$$

and the brackets denote an ensemble average over a (large) mass–complete sample.

PL+LN covariance model for halo signals

1.1 Multivariate Space Density

The space density as a function of the multivariate properties, $\mathbf{s}$, is found by the convolution, $n(\mathbf{s}) = \int d\mu\, n(\mu)\, p(\mathbf{s}|\mu)$. Using equations (1) and (4), the result is

$$n(\mathbf{s}) = \frac{A\Sigma}{(2\pi)^{(N-1)/2}|\Psi|^{1/2}} \exp\left[-\frac{1}{2}(\mathbf{s}^\dagger\Psi^{-1}\mathbf{s} - \frac{\bar{\mu}^2(\mathbf{s})}{\Sigma^2})\right], \quad (6)$$

exact form for multi-signal space density

where Σ^2 is the **multi-property mass variance** defined by

$$\Sigma^2 = (\mathbf{m}^\dagger\Psi^{-1}\mathbf{m})^{-1}, \quad (7)$$

and the mean mass is

$$\bar{\mu}(\mathbf{s}) = \frac{\mathbf{m}^\dagger\Psi^{-1}\mathbf{s}}{\mathbf{m}^\dagger\Psi^{-1}\mathbf{m}} - \alpha\Sigma^2, \quad (8)$$

$$\equiv \bar{\mu}_0(\mathbf{s}) - \alpha\Sigma^2. \quad (9)$$

mean mass selected by signals is biased low (Malmquist bias)

The first term, $\bar{\mu}_0(\mathbf{s})$, is the mean mass for the case of a flat mass function, $\alpha = 0$, which corresponds to the mass expected from inverting the input log-mean relation.

The second term, $\alpha\Sigma^2$, represents the mass shift induced by asymmetry in the convolution when $\alpha > 0$. (Low mass halos scattering up outnumber high mass systems scattering down.) Note that **the magnitude of this effect scales with the variance**, not the rms deviation.

Applying Bayes' theorem in the form $p(\mu|\mathbf{s}) = p(\mathbf{s}|\mu)n(\mu)/n(\mathbf{s})$ leads to the result that the set of masses selected by a specific set of properties is Gaussian in the log with mean given by equation (9) and variance, equation (7).

PL+LN covariance model for halo signals

1.1.1 Explicit expressions for the one-variable case

For a single property, $s \equiv \ln(S)$, with slope, m, and logarithmic scatter at fixed mass, σ, the mass variance at fixed S is

$$\Sigma^2 = \left(\frac{\sigma}{m}\right)^2. \tag{10}$$

The mean mass for a sample complete in S is

$$\bar{\mu}(s) = \frac{s}{m} - \alpha\Sigma^2. \tag{11}$$

The property space density function is

$$n(s)\,ds = (A/m)\,\exp\{-\alpha\left(\frac{s}{m} - \alpha\Sigma^2/2\right)\}\,ds, \tag{12}$$

which is a power-law in the original property, $n(S) \propto S^{-(\alpha/m)}$.

Note that the effective shift in mass, $\alpha\Sigma^2/2$, is half that in the expression above. These expressions are consistent, in that they address different questions. Equation (11) gives the mean ln(mass) of a signal-selected sample while equation (12) gives the ln(mass) value that matches the local space density – in number per volume per ln(S) – of halos with property value, S.

cosmology

astrophysics

PL+LN covariance model for halo signals

1.1.2 Explicit expressions for the two-variable case

For two properties, we introduce the correlation coefficient, $r \equiv \langle \delta_1 \delta_2 \rangle$, of the normalized deviations, $\delta_i \equiv (s_i - \bar{s}_i)/\sigma_i$, and write the covariance matrix,

$$\Psi = \begin{pmatrix} \sigma_1^2 & r\sigma_1\sigma_2 \\ r\sigma_1\sigma_2 & \sigma_2^2 \end{pmatrix},$$

and its inverse,

$$\Psi^{-1} = (1-r^2)^{-1} \begin{pmatrix} \frac{1}{\sigma_1^2} & -\frac{r}{\sigma_1\sigma_2} \\ -\frac{r}{\sigma_1\sigma_2} & \frac{1}{\sigma_2^2} \end{pmatrix}.$$

The mass variance is now a harmonic mixture

$$\Sigma^{-2} = (1-r^2)^{-1}\left(\sigma_{\mu 1}^{-2} + \sigma_{\mu 2}^{-2} - 2r\sigma_{\mu 1}^{-1}\sigma_{\mu 2}^{-1}\right), \tag{13}$$

where $\sigma_{\mu i} = \sigma_i/m_i$ is the mass scatter at fixed signal S_i.

The zero-slope mean mass is

$$\bar{\mu}_0(s_1, s_2) = \frac{(s_1/m_1)\sigma_{\mu 1}^{-2} + (s_2/m_2)\sigma_{\mu 2}^{-2} - r(s_1/m_1 + s_2/m_2)\sigma_{\mu 1}^{-1}\sigma_{\mu 2}^{-1}}{\sigma_{\mu 1}^{-2} + \sigma_{\mu 2}^{-2} - 2r\sigma_{\mu 1}^{-1}\sigma_{\mu 2}^{-1}}, \tag{14}$$

and the **joint space density** is

$$n(s_1, s_2) = \frac{A\Sigma}{\sqrt{2\pi(1-r^2)}\sigma_1\sigma_2} \exp\left[-\alpha\bar{\mu}_0 + \frac{\Sigma^2}{2}\left(\alpha^2 - \frac{(s_1/m_1 - s_2/m_2)^2}{\sigma_{\mu 1}^2\sigma_{\mu 2}^2}\right)\right]. \tag{15}$$

The first two terms in the exponent are analogous to those in the 1D expression, equation (12). For "reasonable" choices of (S_1, S_2) pairs — meaning values that pick out comparable mass scales, $s_1/m_1 \sim s_2/m_2$ — the space density remains effectively power-law. The third term in the exponent suppresses the number density for unreasonable pairings of s_1/m_1 and s_2/m_2, those lying out in the wings of the bivariate Gaussian.

anti-correlated signals best for mass selection

mass scatter for two-property joint selection

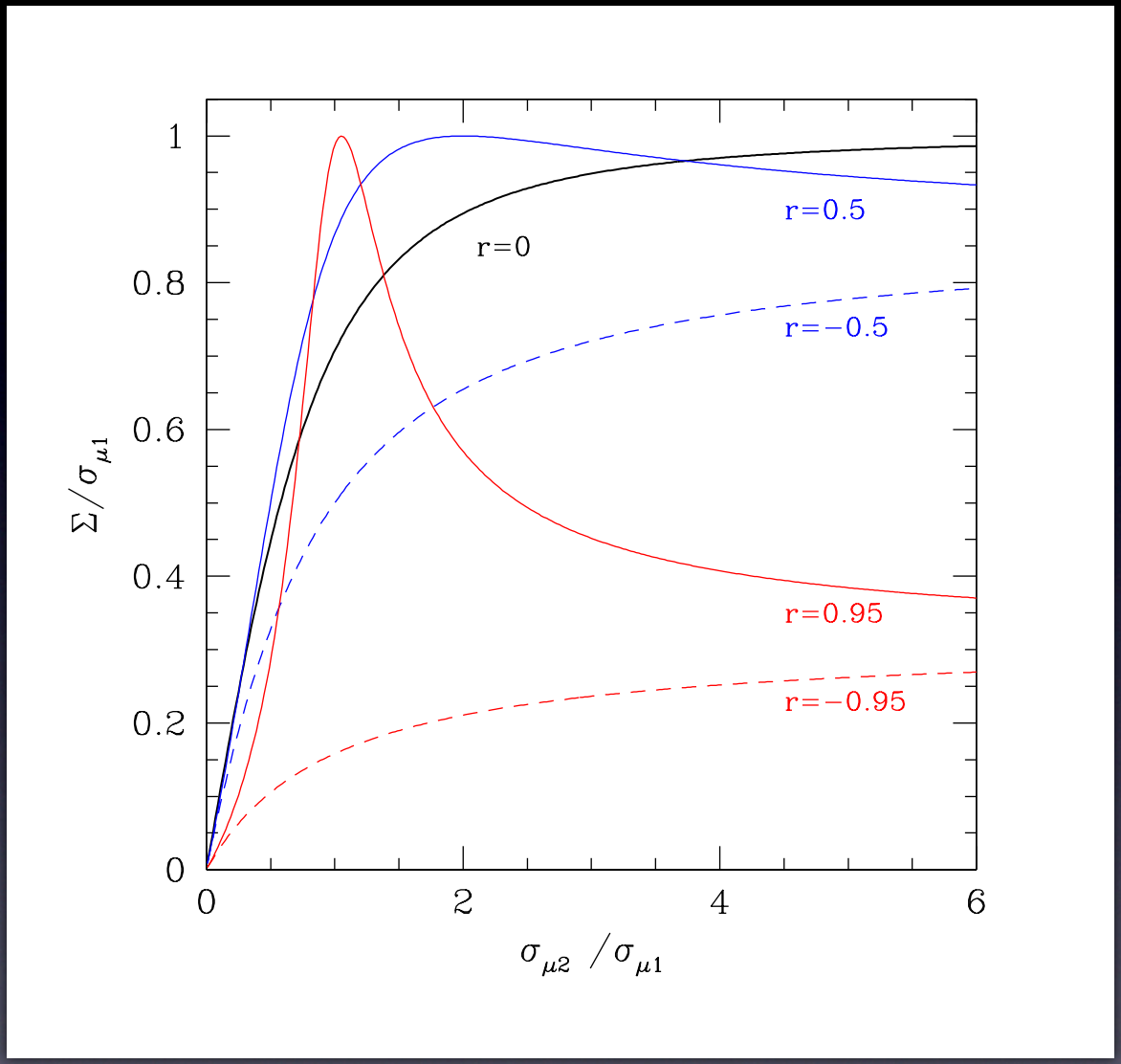

mass scatter for hot gas observables from Millennium Gas Simulations

Allen, Evrard & Mantz 2011
Stanek et al 2010

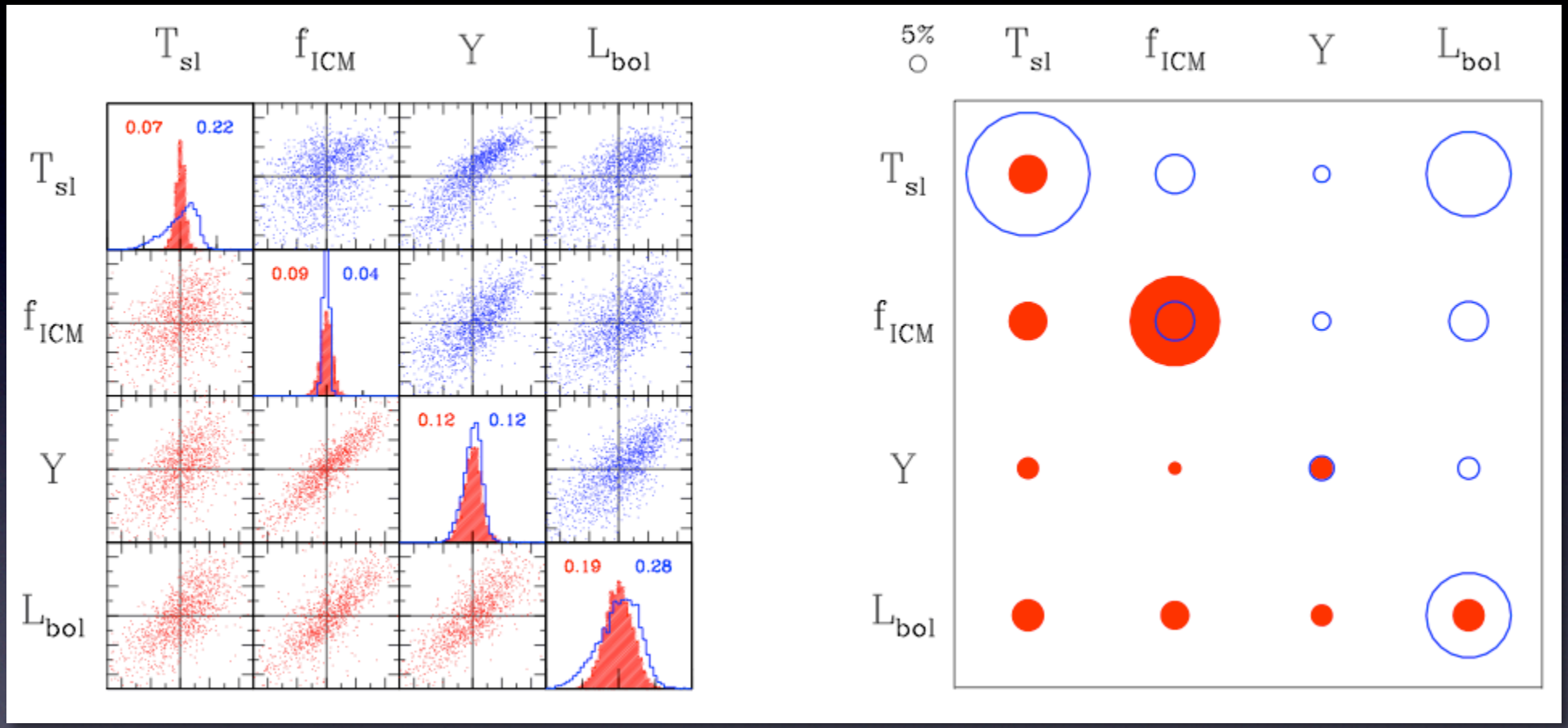

preheating (200 kev-cm^2 @z=4)
gravity only

PL+LN covariance model for halo signals

1.2 Property-selected samples

For a halo sample selected with some property, s_1, we can now use Bayes' theorem to find the joint probability of those halos having a second property, s_2, and mass, μ. The result can be expressed as a bivariate Gaussian in terms of the two-element vector, $\mathbf{t} = [s_2\ \mu]$,

$$p(\mathbf{t}|s_1) \;=\; \frac{1}{(2\pi)|\tilde{\Psi}|^{1/2}} \exp\left[-\frac{1}{2}(\mathbf{t}-\bar{\mathbf{t}})^{\dagger}\tilde{\Psi}^{-1}(\mathbf{t}-\bar{\mathbf{t}})\right], \tag{16}$$

where the mean mass, $\bar{\mu}(s_1)$, is defined by equation (11) and the mean of the non-selection property is given by

$$\bar{s}_2(s_1) \;=\; m_2\left(\bar{\mu}(s_1) + \alpha r \sigma_{\mu 1}\sigma_{\mu 2}\right). \tag{17}$$

Note that, if $r < 0$, the non-selected property mean can be "doubly" biased low relative to a simple $m_2(s_1/m_1)$ expectation, with one shift coming from the extra $(-\alpha\Sigma^2)$ term in the mean mass and the second coming from the second term in the above expression.

The covariance in s_2 and μ at fixed s_1 is given by

$$\tilde{\Psi} = \begin{pmatrix} \sigma_{21}^2 & \tilde{r}\sigma_{21}\sigma_{\mu 2} \\ \tilde{r}\sigma_{21}\sigma_{\mu 2} & \sigma_{\mu 2}^2 \end{pmatrix},$$

where the variance in s_2 at fixed s_1 is

$$\sigma_{21}^2 \;=\; m_2^2\left(\sigma_{\mu 1}^2 + \sigma_{\mu 2}^2 - 2r\sigma_{\mu 1}\sigma_{\mu 2}\right). \tag{18}$$

future program: combine large samples to extract signal covariance

RASS analysis of maxBCG sample

X-ray luminosity in ROSAT All-Sky Survey (RASS) at locations of maxBCG clusters

scatter in Lx at fixed Ngal

Rykoff et al 2008a

$$\sigma_{\ln L_X \mid N_{gal}} = 0.83 \pm 0.03$$

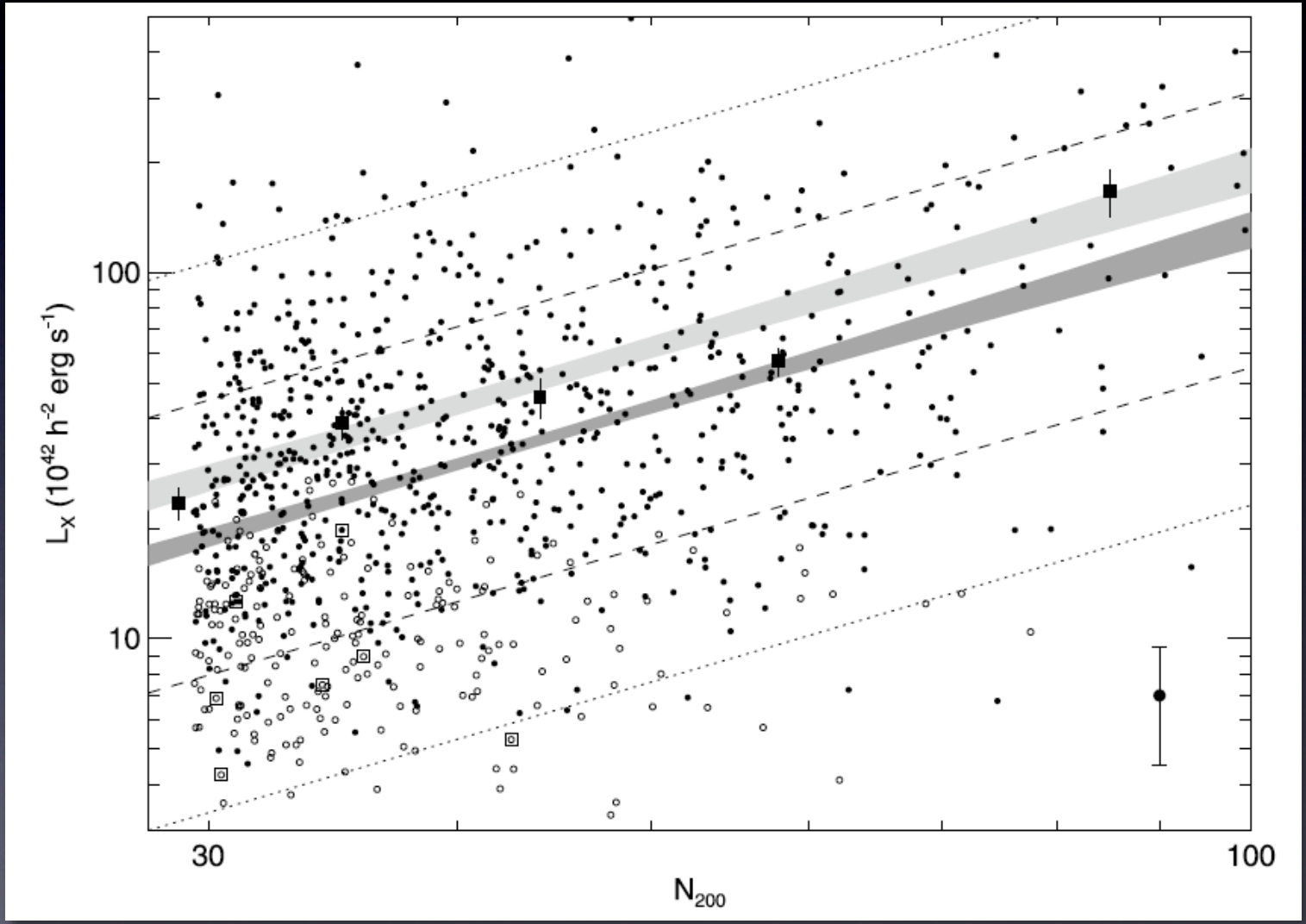

first measurement of property covariance for clusters

Rozo et al 2009

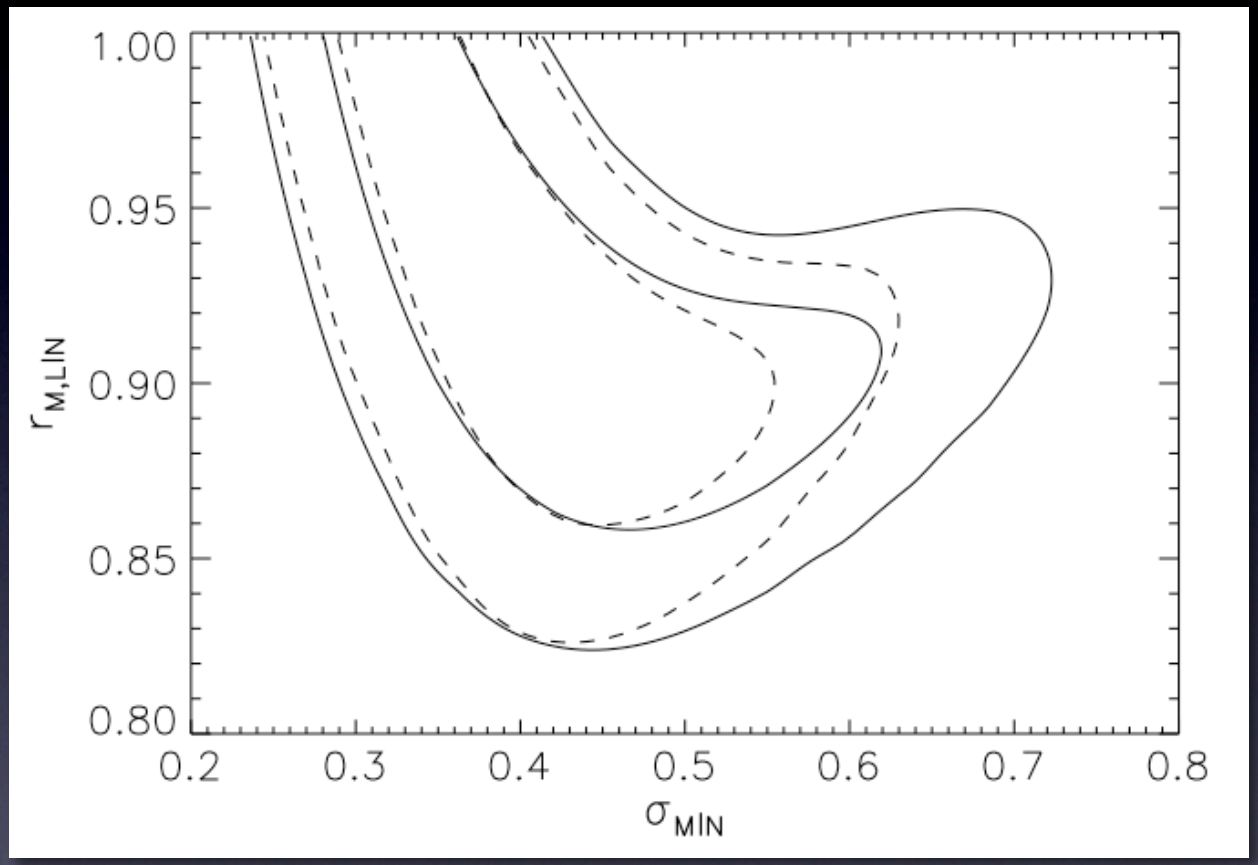

scatter in ln(mass) at fixed Ngal

From SDSS-RASS:

- $dn(N_{200})/dN_{200}$
- L_X–N_{200} scaling
  slope, norm, scatter
- M_{200}–N_{200} scaling
  slope, norm

missing:

M_{200}–N_{200} scatter

M_{200}, L_X | N_{200} correlation

Extra information:

400d survey

L_X –M_{500} scaling
slope, norm, scatter

Vikhlinin et al 2008

PL+LN covariance model for halo signals

expect large covariance if optical selection has larger mass scatter than X-ray

The s_2–mass correlation coefficient, $\tilde{r}$, depends on both the intrinsic property correlation, r, as well as the ratio of scatter in mass for the two properties,

$$\tilde{r} = \frac{\sigma_{\mu 1}/\sigma_{\mu 2} - r}{\sqrt{1 - r^2 + (\sigma_{\mu 1}/\sigma_{\mu 2} - r)^2}}. \quad (19)$$

If the selection property is an excellent mass proxy ($\sigma_{\mu 1} \to 0$), then $\tilde{r} \to -r$.

If the selection property is a much poorer mass proxy compared to the second property, then $\tilde{r} \to 1$, irrespective of the intrinsic correlation, r.

benefits of large, overlapping cluster samples

1. Test basic model component with cross-signal abundance matching
   – e.g., true halo mass for Nth-ranked cluster identified with signal 1 must agree with the estimate for a sample selected with signal 2

2. Constrain signal covariance at fixed halo mass
   – mean and variance of signal 2 binned in signal 1

3. Astrophysical models make explicit joint signal predictions
   – e.g., $\langle \ln Y_{SZ} \rangle$ should dependent linearly on $\langle \ln M_{gas} \rangle$ and $\langle \ln T_X \rangle$

role of LSS simulations in dark energy studies

basic steps to study dark energy (DE) with large-scale structure

1. produce a large survey of a class of cosmic objects to $z \geq 1$, using a class that enables statistical tracing of dark matter
   – extract statistics, $\mathbf{y}_i$, for DE test method *i* (e.g., BAO, WL, CL)

2. compute model expectations for object survey statistics
   – calculate likelihood, $p(\mathbf{y}_i \mid \theta, \alpha)$, over cosmological params, θ, and within an assumed astrophysical model, α, for the specific object class use

3. perform the likelihood analysis, marginalizing over (or just fixing) α
   – extract cosmological constraints, $p(\theta)$

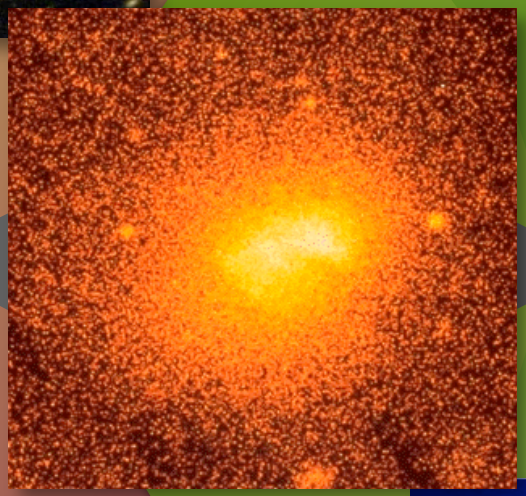

astrophysics

cosmology

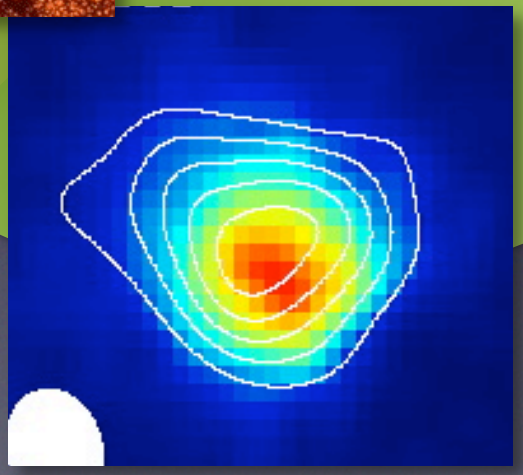

role of simulations in DE survey science

Survey-specific simulations enable ***key capabilities:***

* to extract unbiased statistical signals, $\mathbf{y}_i$, from the raw object catalog

* to predict statistical expectations, $p(\mathbf{y}_i \mid \theta, \alpha)$ for a variety of models

* to calculate the expected signal covariance, $\mathrm{COV}(\mathbf{y}_i , \mathbf{y}_j)$

Dark Energy Survey (DES) is nearly ready for first light

An NSF+DOE-funded study of dark energy using four techniques

1) Galaxy cluster surveys (with SPT)
2) Galaxy angular power spectrum
3) Weak lensing/cosmic shear
4) SN Ia distances

Two linked, multiband optical surveys

5000 deg^2 *g r i z Y* bands to ~24th mag in r
Repeated observations of 40 deg^2

Development and schedule

Construction: 2007-2011
- New 3 deg^2 camera on Blanco 4m, Cerro Tololo
- Data management system at NCSA

Survey Operations: 2012-2016
- 510 nights of telescope time over 5 years

John Peoples, Director

Fermilab, U Illinois, U Chicago, LBNL, U Michigan
CTIO/NOAO, Barcelona, UCL, Cambridge, Edinburgh

DES Simulation Working Group: **Blind Cosmology Challenge**

3M SU TeraGrid-XSEDE allocation (TACC ranger) + 120 Tb storage (IU HPSS)

6-12 cosmological models

– full sky surveys of DM structure to z~6 (variable mass rez.)
built from four 2048^3 N-body sims. of nested volumes (1-6 Gpc/h)

+ empirically-tuned galaxy catalog, ADDGALs (R. Wechsler, M. Busha)

+ weak lensing shear (M. Becker)

+ synthetic image generation for ~200 sq deg including multiple detector-telescope-sky effects (H. Lin)

source code to be made available on bitbucket repository

GOALS:

* validate science pipelines used by DE science teams
* provide testbed for characterizing systematic error sources
* assist planning for follow-up observations

Cosmic Sky Machine (COSMA)

DARK ENERGY SURVEY

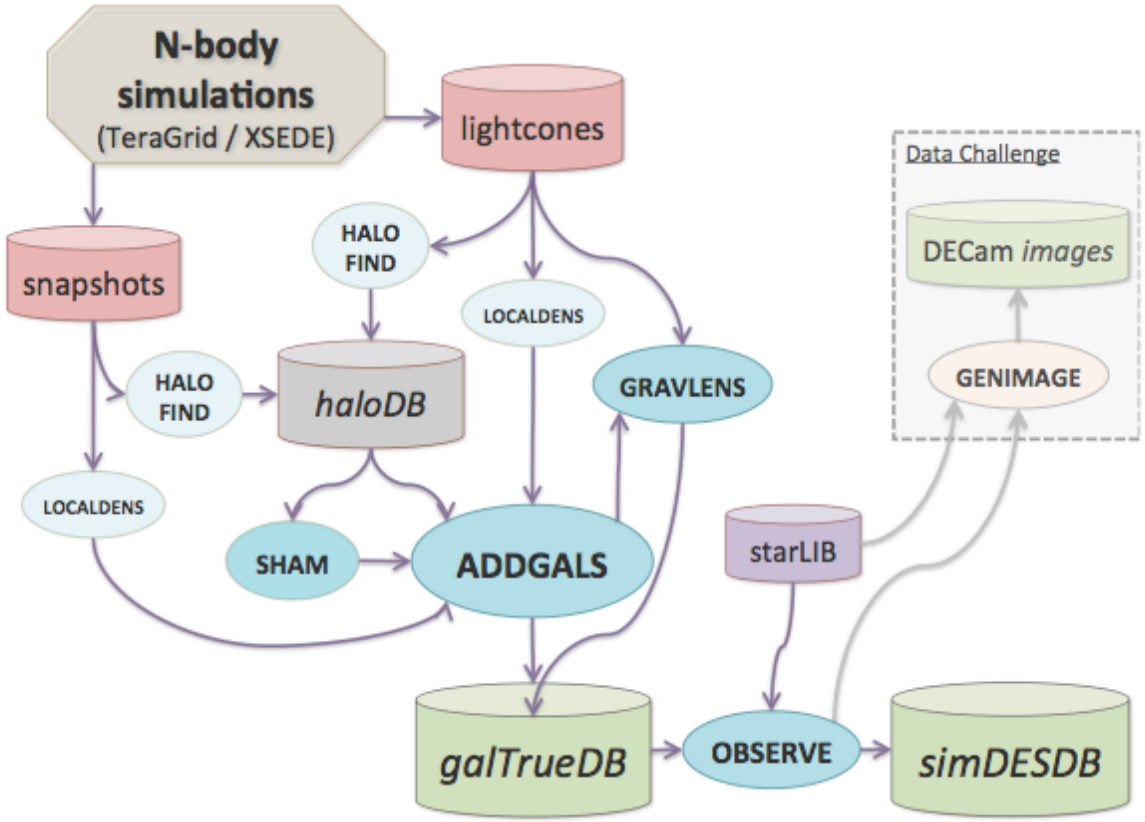

Catalog Simulations

M. Becker (Chicago)
M. Busha (Zurich)
B. Erickson (Michigan)
A. Evrard (Michigan)
A. Kravtsov (Chicago)
R. Wechsler (Stanford)

Image Simulations

H. Lin (Fermilab)
Nikolai Kuropatkin (Fermilab)
+ DES Data Management

simulation workflow to support DES analysis

Risa Wechsler, DES Penn Collaboration Mtg, 11 Oct 2011

BCC simulation pipeline

1. Decide on a cosmological model (first one WMAP7. rest TBD.)
2. Initial conditions, run simulation, output light cone, run halo finder, validate (Busha, Erickson, Becker)
3. Add galaxies (Busha, Wechsler)
4. Run validation tests (Hansen, Busha, Wechsler, others)
5. Calculate shear at all galaxy positions (Becker)
6. Add shapes, lens (magnify & distort) galaxies (Dietrich)
7. Add stars (Santiago)
8. Determine mask (Swanson), including varying photometric depth & seeing, foreground stars
9. Blend galaxies (Hansen)
10. Determine photometric errors (Busha, Lin), incorporating mask information
11. Misclassify stars and galaxies (Sevilla, Hansen, Santiago)
12. Determine photometric redshifts (Busha, Cunha, Gerdes, etc)
13. Provide a lensed galaxy catalog in the DESDM database with:

ra, dec, mags, magerrors, photoz's, p(z), size, ellipticity, star/galaxy probability, seeing

☆ grey steps already implemented in v3.02 (220 sq. degrees) and/or for BCCv0.1

☆ **Science working groups do analysis!**

simulation workflow to support DES analysis

Risa Wechsler, DES Penn Collaboration Mtg, 11 Oct 2011

BCC "observed" information

Available now for v3.02

- `RA`: Right ascension (lensed).
- `DEC`: Declination (lensed).
- `MAG_[UGRIZY]`: The observed DES magnitudes with photometric errors applied to LMAG.
- `MAGERR_[GRIZY]`: Estimated photometric errors for each band.
- `EPSILON`: Observed ellipticity.
- `SIZE`: Observed size (FLUX_RADIUS).
- `PGAL`: Probability that the object is a galaxy.
- `PHOTOZ_GAUSSIAN`: Estimated photo-z using a gaussian PDF with $\sigma = 0.03/(1+z)$.
- `ZCARLOS`: Redshift estimate from zCarlos code.
- `PZCARLOS`: ARRAY of $p(z)$ in bin of $\Delta z = 0.02$.
- `ARBORZ`: Redshift estimate from ArborZ code.
- `ARBORZ_ERR`: Redshift errorestimate from ArborZ code.
- `PZARBOR`: ARRAY of $p(z)$ in bin of $\Delta z = 0.032$.
- `ANNZ`: Redshift estimate from ANNz code.
- `ANNZ_ERR`: Redshift error estimate from ANNz code.

+ vista magnitudes

- Is there additional information we should be providing?

HEALPix-based map of DC6B 200 deg^2 convergence and shear fields

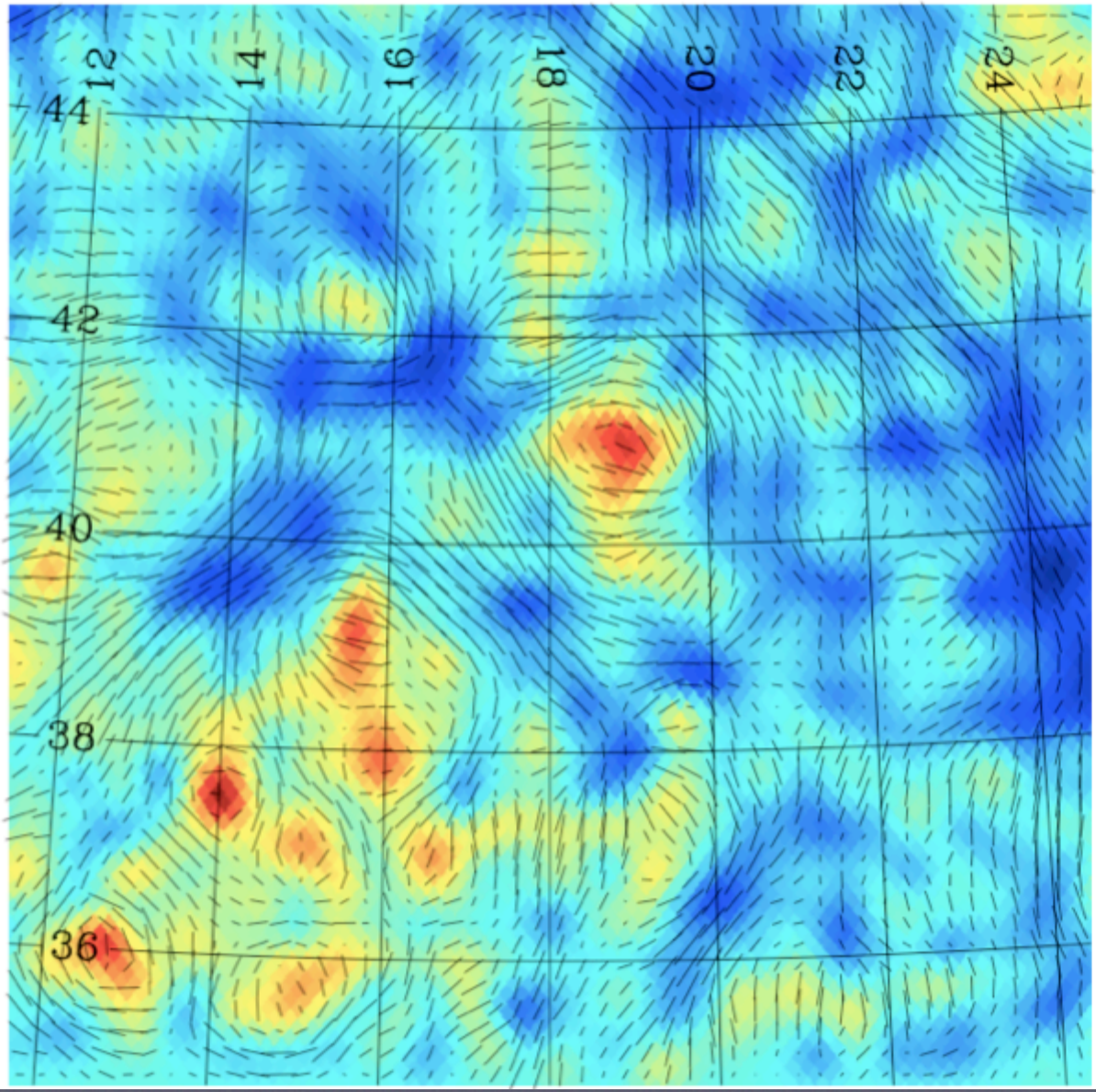

Colors indicates convergence ∝ surface mass density; redder ⟹ higher density

Black "whiskers" show shear field due to gravitational lensing

Figure from M. Becker

courtesy H. Lin (FNAL)

Close-up of raw simulated images

Note bright star artifacts, cosmic rays, cross talk, glowing edges, flatfield ("grind marks", tape bumps), bad columns, 2 amplifiers/CCD

DARK ENERGY SURVEY

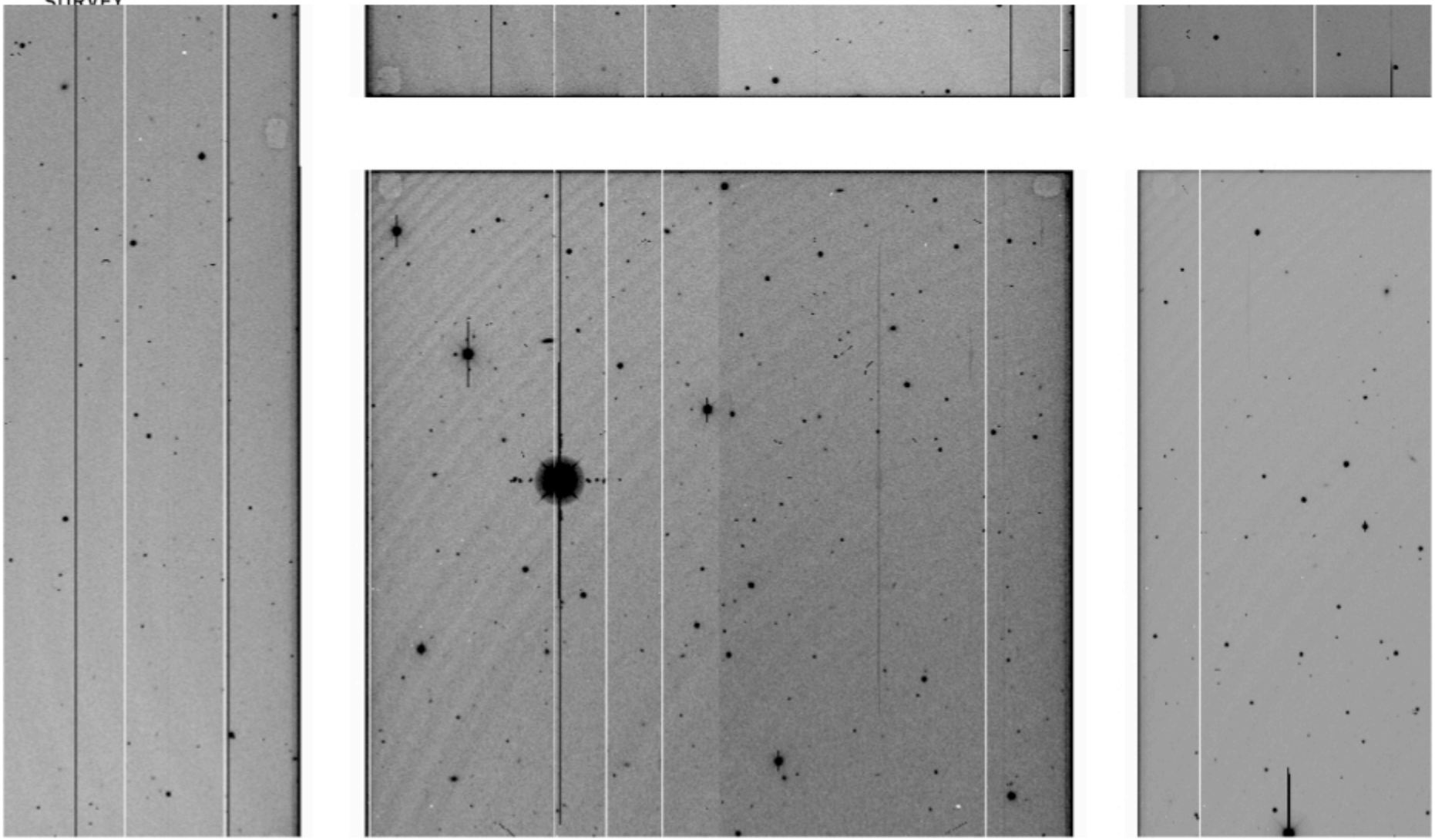

courtesy H. Lin (FNAL)

Example DC6B image using profile galaxies: Part of raw r-band image of one CCD

DARK ENERGY SURVEY

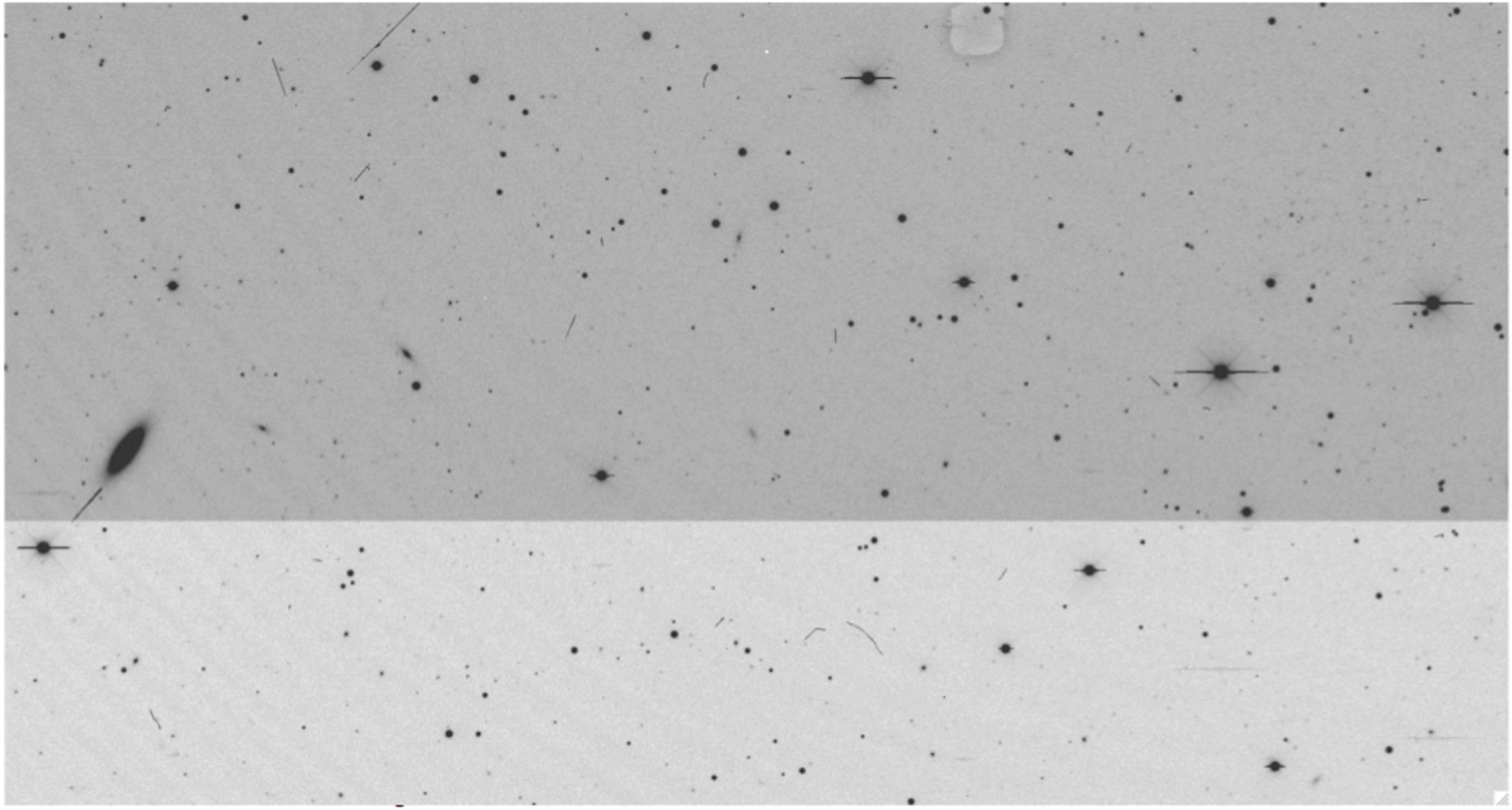

courtesy H. Lin (FNAL)

DARK ENERGY SURVEY

Same r-band image after bias subtraction and flatfielding (cosmic rays can be removed but left in here)

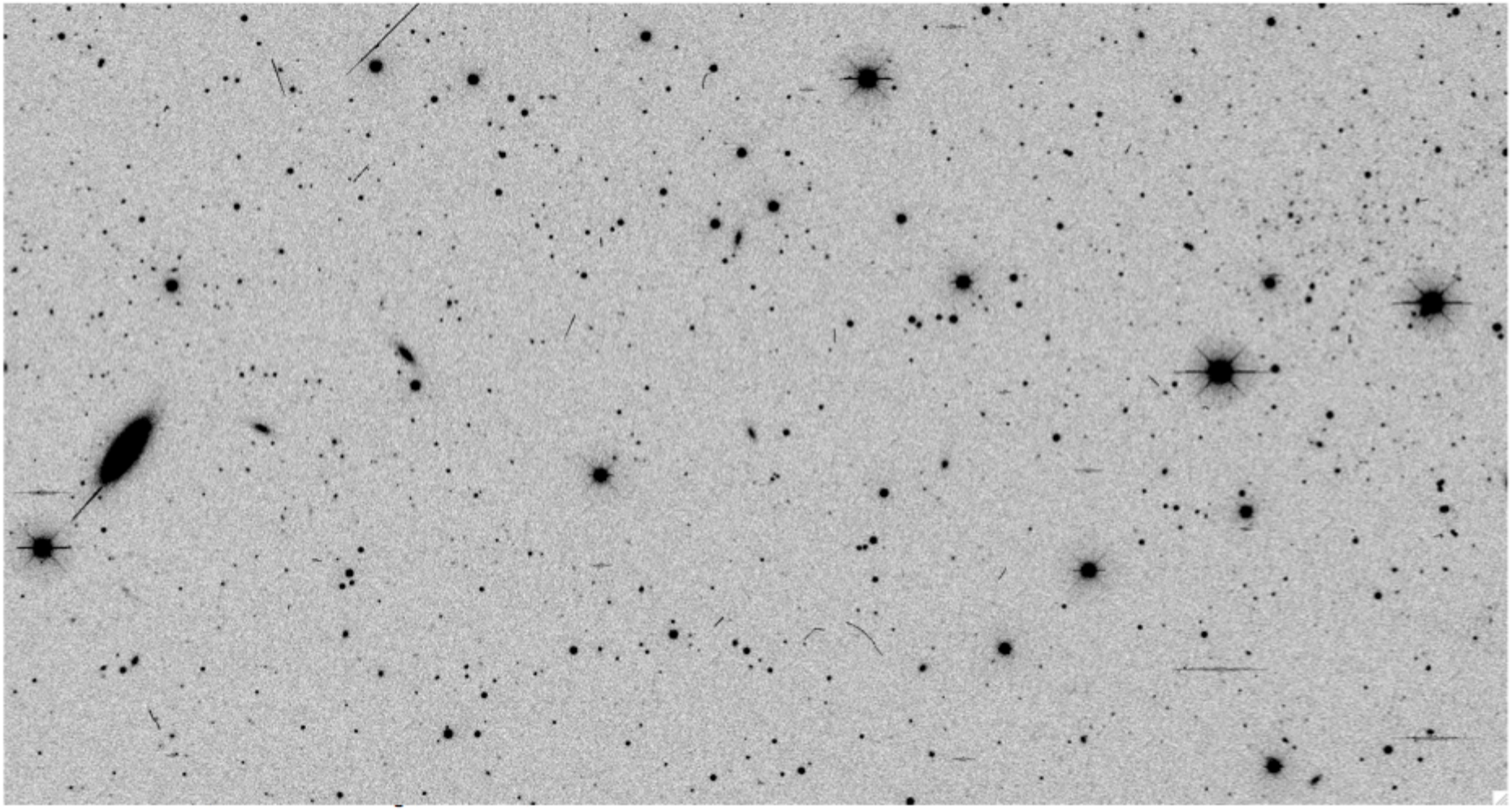

courtesy H. Lin (FNAL)

DARK ENERGY SURVEY

Same area shown as color composite of separate images in g,r,i filters

(note distinct color of rich galaxy cluster at upper right)

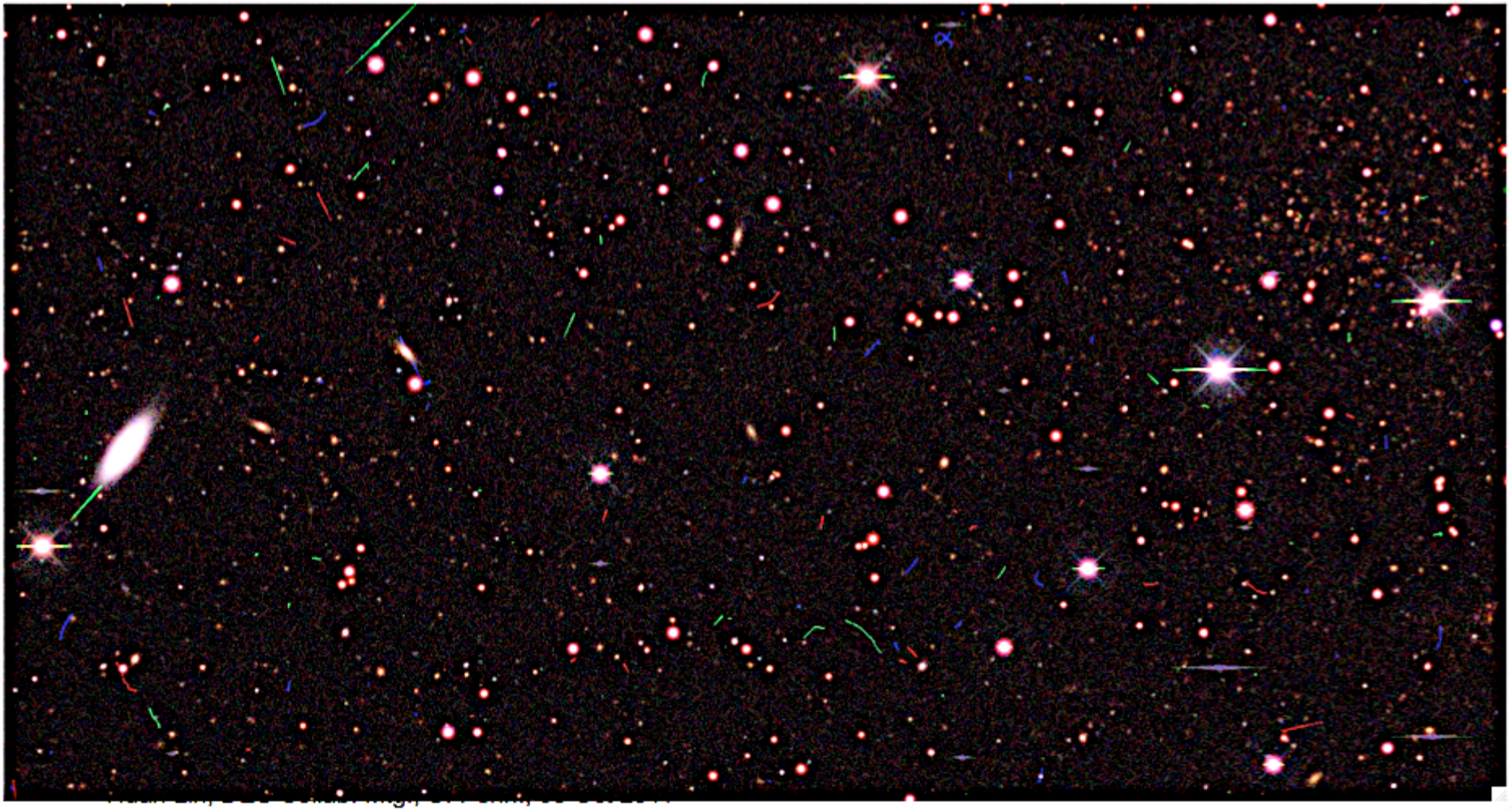

calibration of halo lensing mass estimates

Becker & Kravtsov 2011

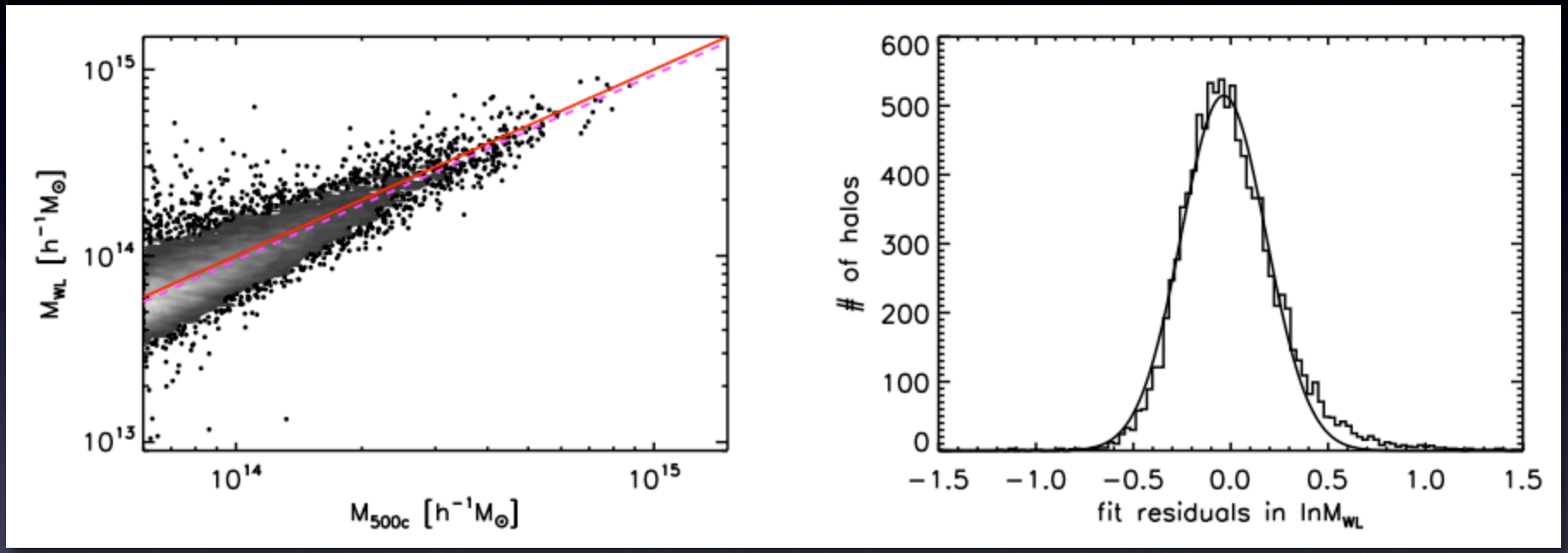

cluster cosmology:

solidifying theoretical framework

- halo space density (well-calibrated functional form)
- halo spatial clustering (")
- multi-component signal model (power-law + log-norm scatter)
- growing body of empirical evidence to inform models
- improving fidelity of simulations

challenges to survey analysis

- survey-specific halo selection
- detailed form of mass-observable relations
- absolute calibration of cluster masses
- sensitivities to baryon physics (feedback)

optical surveys for BAO & WL get clusters "for free"!

large, multi-wavelength surveys are coming

Thank you!

and thanks to Tarun and Subha
for organizing a great school!